



Graz University of Technology
Faculty of Civil Engineering
Institute of Hydraulic Engineering and Water Resource Management

Velocity measurements of approach flow to low head run-off hydropower plant intakes in the laboratory

MASTER'S THESIS

Ulrich ROTH

Submitted to obtain the academic degree

Diplom-Ingenieur

Master's Degree Programme Geotechnical and Hydraulic Engineering

Graz, January 2018

Advisor of the thesis:

Ass.Prof. Dipl.-Ing. Dr.nat.techn. Josef SCHNEIDER

Further advisor:

M.Sc. Shervin SHAHRIARI

Eidesstattliche Erklärung

Ich erkläre an Eides statt, dass ich die vorliegende Arbeit selbstständig und ohne fremde Hilfe verfasst, andere als die angegebenen Quellen/Hilfsmittel nicht benutzt und die den benutzten Quellen wörtlich und inhaltlich entnommenen Stellen als solche kenntlich gemacht habe. Das in TUGRAZonline hochgeladene Textdokument ist mit der vorliegenden Masterarbeit identisch.

Graz, im Jänner 2018

.....

Statutory Declaration

I declare that I have authored this thesis independently, that I have not used other than the declared sources/resources, and that I have explicitly marked all material which has been quoted either literally or by content from the used sources. The document uploaded in TUGRAZonline is identical with the present master's thesis.

Graz, January 2018

.....

Acknowledgement

Firstly I would like to express my gratitude to all the members of the Institute of Hydraulic Engineering and Water Resources Management who assisted and supported me during the whole time I worked on my master's thesis.

Particularly I would like to thank the laboratory staff who helped me to set up and run my experiments in the hydraulics laboratory. Furthermore, I would like to convey my gratefulness to Ass.Prof. Dipl.-Ing. Dr.nat.techn. Josef Schneider who corrected and marked my thesis. Also I would like to mention my appreciation to M.Sc. Shervin Shahriari who was of particular importance for my work and always was willing to help me with emerging issues.

Many thanks go to all of my student colleagues and good friends who came along with me through university and lived with me through all the ups and downs of a student life.

Words are powerless to describe my gratitude to my parents and my sister who were there for me my whole lifetime and accompanied me from the very beginning. They always supported me, financially and emotionally, and their advices helped me to make the most out of my dreams.

Kurzfassung

In der Welt des Wasserbaus kommt es bei den meisten Projekten aufgrund ihrer Größe und ihres enormen finanziellen Aufwandes zu umfassenden Planungs- und Berechnungsschritten. Dazu zählen in den meisten Fällen auch Untersuchungen in wasserbaulichen Labors, welche das Bauwerk in einem Maßstab nachbilden und eine Übertragung der daraus gewonnenen Erkenntnisse auf den Prototypen ermöglichen. Diese Arbeit befasst sich genau mit solchen Messungen an dem Kraftwerksmodell Gratkorn, im Speziellen mit Geschwindigkeitsmessungen im Stauration und im Anströmbereich der Turbinen.

Diese Masterarbeit setzt sich mit Acoustic-Doppler-Velocimetry Geschwindigkeitsmessungen und ihren Funktionen und Anwendungsbereichen im Labor auseinander. Nach einer umfassenden Literaturrecherche werden die genauen Einstellungen des Messgeräts für die Messungen am Modell Gratkorn mittels Testmessungen in einem Glasgerinne ermittelt. Hierbei wird versucht Bereiche mit Messungenauigkeiten zu identifizieren und zu eliminieren. Am Modell Gratkorn wird das Anströmverhalten der Turbinen untersucht, verschiedene Geschwindigkeitsprofile im Oberwasser erstellt und die im Bereich der Geschiebeleitschwelle entstehenden Fließgeschwindigkeitsveränderungen genau erfasst. Die Messungen zeigen eine ungleichmäßige Anströmung der linken Turbine aufgrund der Geschiebeleitschwelle und des Trennpfeilers. Der Wasserstrom zur rechten Turbine hingegen ist viel gleichmäßiger, der Einfluss der baulichen Maßnahmen an der Flusssohle äußerst gering. Die Geschwindigkeitsverteilung im Stauration beschreibt eine gewisse Sogwirkung zu den Turbinen hin und nahezu stehendes Wasser direkt vor den äußersten beiden Wehrfeldern. Des Weiteren zeigen die Ergebnisse den Einfluss der Geschiebeleitschwelle auf das Strömungsverhalten bis zu einer Entfernung von nahezu 75 m oberwasserseitig der Wehrachse.

Schlagwörter: Acoustic Doppler Velocity Messungen, Modellversuche, Turbulenz, Froude's Gesetz, Vectrino, WinADV

Abstract

In the world of hydraulic engineering most projects, due to their size and their enormous financial effort, need comprehensive planning and calculation steps. In most cases this includes tests in hydrotechnical laboratories where the building is recreated in a scale factor and the calculated results are compared to the results in the laboratory test. This thesis deals with such measurements at the hydropower plant model Gratkorn, in particular with velocity measurements in the storage area and in the flow field of the turbines.

This master's thesis focuses on Acoustic-Doppler-Velocimetry measurements and their functions and applications in the laboratory. After a comprehensive literature research the exact settings of the device for the measurements at the model Gratkorn are determined by means of several tests in a flume. Areas with measurement inaccuracies are tried to be identified and eliminated. On the model Gratkorn the approach flow behaviour to the turbines is investigated, speed profiles in the upstream area are created and the velocity differences in the area of the sediment control bedplate were captured exactly. The results describe an uneven water flow distribution towards the left turbine because of the sediment cut-off wall and the separation pillar. The water flow to the right turbine is uniformly distributed; the influence of the constructional measures on the river bed is minimal. The velocity distribution in the storage area is characterized by a vortex towards the turbines and nearly no water movement directly upstream of the exterior two weirs. Furthermore, the influence on the water flow of the sediment cut-off wall is recognisable up to a distance of nearly 75 m upstream from the weir axis.

Keywords: Acoustic Doppler Velocity measurement, laboratory models, turbulence, Froude's law, Vectrino, WinADV

Table of Contents

Eidesstattliche Erklärung.....	i
Statutory Declaration.....	i
Acknowledgement.....	ii
Kurzfassung.....	iii
Abstract.....	iv
Table of Contents.....	v
1. Acoustic - Doppler - Velocity Measurements	1
1.1 Introduction.....	1
1.2 Objective.....	2
1.3 History of Acoustic Doppler Velocity Measurements	3
1.4 Acoustic Doppler Velocimeter in the laboratory of the Institute of Hydraulic Engineering and Water Resources Management	7
2. General	10
2.1 Operating principle of the Acoustic - Doppler - Velocimeter	10
2.1.1 Configurations.....	14
2.1.2 Troubleshooting	20
2.2 WinADV-Post-Processing	26
2.3 Recapitulation	31
3. ADV - Measurements in a laboratory flume	33
3.1 Set-up of measurement	33
3.2 Results.....	36
3.3 Improvement / Modification	41
4. Laboratory Model Gratkorn	42
4.1 From hydropower plant Gratkorn to model Gratkorn	42
4.2 Approach flow to turbines.....	45
5. ADV - Measurements at the model Gratkorn	48

5.1	Turbines 1 and 2.....	50
5.1.1	Description of turbines 1 and 2.....	50
5.1.2	Results of turbine 1	51
5.1.3	Results of turbine 2	54
5.2	Profile PR A - OW	58
5.2.1	Description of profile PR A - OW	58
5.2.2	Results of profile PR A - OW	60
5.3	Profile PR B – OW	63
5.3.1	Description of profile PR B - OW	63
5.3.2	Results of profile PR B – OW	63
5.4	Profile PR 0.1 - OW	66
5.4.1	Description of profile PR 0.1 - OW.....	66
5.4.2	Results of profile PR 0.1 – OW.....	66
5.5	Profile PR 1.0 - OW	69
5.5.1	Description of profile PR 1.0 - OW.....	69
5.5.2	Results of profile PR 1.0 - OW	69
5.6	Profile PR 1.1 - OW	72
5.6.1	Description of profile PR 1.1 - OW.....	72
5.6.2	Results of profile PR 1.1 - OW	72
5.7	Profile PR 2.0 - OW	75
5.7.1	Description of profile PR 2.0 - OW.....	75
5.7.2	Results of profile PR 2.0 - OW	75
5.8	Profile PR 2.1 - OW	78
5.8.1	Description of profile PR 2.1 - OW.....	78
5.8.2	Results of profile PR 2.1 - OW	78
5.9	Horizontal contour of velocity	81
6.	Conclusion and perspective	84
6.1	Conclusion.....	84
6.2	Perspective	85
	List of references.....	86
	List of figures.....	89
	List of tables	92
	Appendix	93

1. Acoustic - Doppler - Velocity Measurements

1.1 Introduction

In hydraulic engineering water flows play an important role for the functioning of essential parts of a hydraulic structure. These flows are very complex mechanisms which are difficult to understand and describe. Most of the time simplifying problems and use of common assumptions do not lead to satisfying results. Furthermore, the vast majority of simulation programs for hydraulic problems are very complex and need plenty of computing power to simulate water flow. Even if powerful computers are used, the simulation may need a few hours to be solved. This solution then should be validated with investigations on laboratory models. If just a few parameters of the input are changed (e.g. the discharge is different every day/month), the whole output will be completely different. So if numerous different scenarios should be calculated the computing time will increase enormously. That is one reason why hydraulic laboratories build the hydraulic structures in a scale and run the different load cases. Once a model is built, it can be used for a long time and various studies can be done on this model. Another reason might be the easy modifiability of several parts of such models to find the ideal architecture of important components of these hydraulic structures.

In the hydraulic laboratory at the Institute of Hydraulic Engineering and Water Resources Management of the TU Graz such model tests are carried out. More than 350 various model tests have been performed since the beginning of the laboratory and emergent issues about spillways, bottom outlets, surge tanks, fish passes and run off power plants have been solved [1]. The model Gratkorn is one of the present models in the laboratory. At this model, tests at the inlet structures of the turbines were done to determine the best shape of the cut-off wall and the separation pillar besides others. These tests had to be done to generate an optimum approach flow to the two turbines. The first planned version was modified five times and the last version was specified as the best possible solution for this specific problem [TU Graz]. This latest version of the model Gratkorn is present in the laboratory of the institute and in Figure 1.



Figure 1: Laboratory model Gratkorn

1.2 Objective

The aim of this master's thesis is to perform velocity measurements in the upstream storage area of the model Gratkorn and to evaluate the findings. These velocity measurements are carried out with an Acoustic-Doppler-Velocimeter (ADV) from the company Nortek AS. At first a comprehensive literature research is performed. The next step is a test measurement in a glass channel to check the right settings and the functions of the device. Afterwards the velocities at the intakes of the two turbines in the model Gratkorn are measured. Additional several cross sections in the reservoir upstream of the structure are investigated. Special attention lies on the area between the weir field and the turbine because in this area turbulences occur and the approach flow to the turbines is dissimilar. For the measurements, both turbines are working under full load and the maximum operation level is reached. Other load cases (e.g. malfunction/revision of one turbine, different levels of storage water) are not covered in this thesis. The results of the measurements are processed and velocity contour plots of the cross sections and the layout are generated and discussed.

1.3 History of Acoustic Doppler Velocity Measurements

Acoustic Doppler Velocimetry (ADV) is a measurement technique based on the Doppler shift effect. This effect was discovered by Christian Doppler, an Austrian physicist. His discovery took place in Prague 1842 when he wanted to find evidence for planets moving towards or away from the earth. Basically he found out that this effect is the apparent change in frequency or wavelength of a wave or another periodic event for an observer when the source of waves is moving relative to the observer or the observer is moving relative to the source of waves. Simply speaking that means when an emitting source of waves is moving towards you, the sound you hear is completely different than from the same emitting source when it is moving away from you. The reason why this happens is because the emitter is also moving and so the waves will be either closer together or further apart. So the Doppler effect occurs from either motion of the source of waves or motion of the observer. The frequency, of the emitted waves, does not actually change but the wavelength is affected by the motion and as a consequence the observed frequency is also affected. The Doppler effect is valid for acoustic (sound) and optical (light) waves [2] [3].

Figure 2 shows a schematic representation of the Doppler effect where the source of waves is in motion.

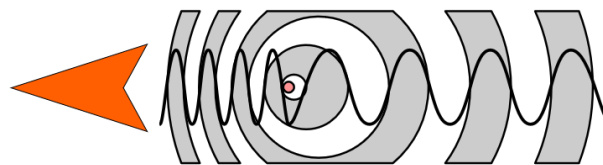


Figure 2: Doppler effect [2]

An interesting result of the Doppler effect is that when the source of sound is moving towards the observer at twice the speed of sound, a piece of music will be recognized in the right tune and correct time, but backwards [3].

In everyday life the Doppler effect can be recognized when vehicles with sirens (e.g. police, ambulance and fire-fighter) drive past or when a train passes by.

Other fields of applications are astronomy, radar, medical imaging and blood flow measurement, satellite communication, temperature measurement, vibration measurement, audio and developmental biology. In the field of hydraulic engineering the Doppler effect is used for velocity profile measurements (Ultrasonic Doppler Velocimetry, UDV) and for flow measurements (Laser Doppler Velocimeter, LDV and Acoustic Doppler Velocimeter, ADV) [2] [3].

For this master's thesis ADV measurements are carried out in the laboratory. The Acoustic Doppler Velocimeter (ADV) is used to measure the velocity of scattering material in the water. The particle velocity is assumed to be the same as the water flow velocity and therefore there should be a homogenous distribution of the particles. Strictly speaking this means that the source of waves is at rest in this case and the observer, in this case reflectors, is moving. The frequency of the emitted waves stays the same but the reflected waves return in closer intervals when the particles are moving towards the Velocimeter probe. This is a short overview how the ADV measurement works; a more detailed explanation is described later (chapter 1.4 and 2.1) [4].

Figure 3 shows a common Velocimeter probe. The main parts of such a probe are the cable, the conditioning module and the measuring probe (from left to right).



Figure 3: Velocimeter [9]

The measuring probe is the part which is submerged into the water and measures the velocity of the particles in the water. The probe consists of one transmitter and between two and four receivers, depending on how many dimensions should be measured (one to three dimensional). The sampling volume is located typically between 5 and 10 cm away from the transmitter (see Figure 4) to guarantee undisturbed measurements and it can be imagined as a cylinder, even though that is a simplistic view [5].

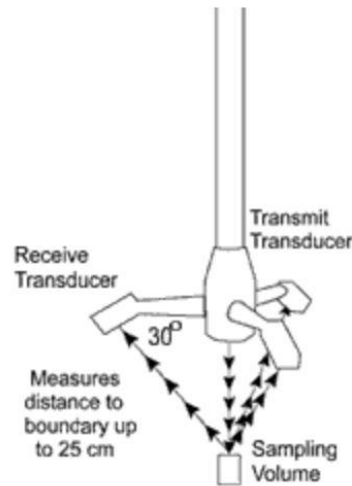
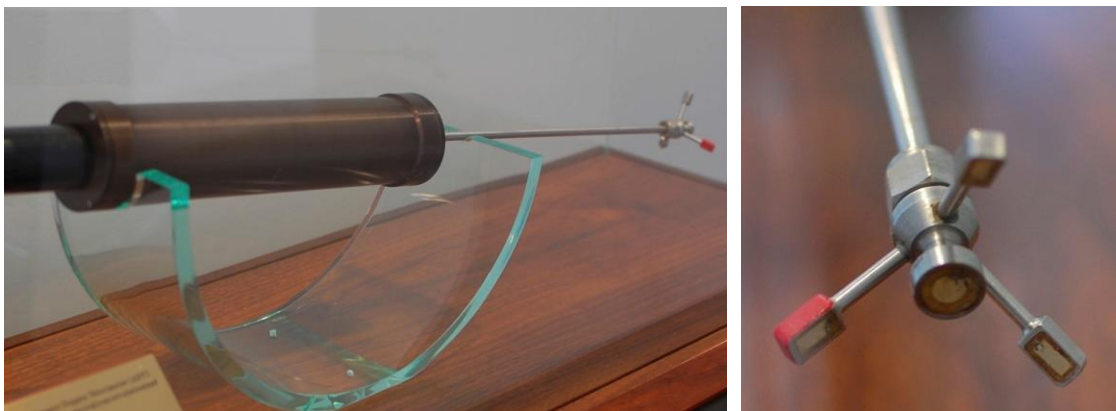


Figure 4: Acoustic sensor [9]

The history of ADV measurements is very young compared to other velocity measurement devices. As described above the Doppler effect was discovered in 1842 but the application for flow measurement devices took nearly 150 years to be invented. In 1984 *Lhermitte R.* and *Serafin R.* published their work of *Pulse-to-pulse coherent Doppler sonar signal processing techniques* in the *Journal Of Atmospheric And Oceanic Technology*. In 1990 *Stanton T. P.* did oceanic turbulence measurements with a coherent bi-static acoustic Doppler profiler. He announced his findings at the 119th Meeting of the Acoustical Society of America. The first prototype of an Acoustic Doppler Velocimeter (see Figures 5 and 6) was built 1993 and after initial tests the ADV revolutionized the way of water velocity measurements [7, slide 4].



Figures 5 and 6: Original ADV [7]

In 1994 *Lhermitte R.* and *Lemmin U.* published their work on *Open-channel flow and turbulence measurement by high resolution Doppler sonar*. Also in 1994 a new acoustic meter for measuring 3D laboratory flows was introduced by *Kraus N. C.*, *Lohrmann A.* and *Cabrera R.* They also published their work on *Acoustic-Doppler-Velocimeter (ADV) for Laboratory Use* in 1994. They described the fundamentals and advancements in hydraulic measurements and experimentation. In 1996 the *Nortek AS* was founded and the *Nortek NDV* introduced. This company is mentioned here because the device used for the laboratory measurements at the institute is a *Nortek Vectrino+*. In 1999 *Snyder W.* and *Castro I.* released their paper on *Acoustic Doppler velocimeter evaluation in stratified towing tank*. In the same year Nortek introduced their *Nortek Vector*. Finally in the year 2005 the *Nortek Vectrino* was introduced and the *Nortek Vectrino+* is a further development of this device. In 2011 the *Nortek Vectrino II* debuts and the *Nortek Vectrino Profiler* is introduced. The *Nortek Vectrino II* is the latest offered version of an Acoustic Doppler Vectrino [7, slide 4].

1.4 Acoustic Doppler Velocimeter in the laboratory of the Institute of Hydraulic Engineering and Water Resources Management

The ADV device used at the institute is a Vectrino+ from Nortek AS. The Vectrino is a high resolution acoustic velocimeter and it can be used in the laboratory and in natural waters and oceans. It measures three dimensional water velocities using the Doppler shift effect. There are many ways of measuring the Doppler effect but Nortek uses a narrowband autocovariance method because it is robust, reliable and accurate [8].

The Nortek Vectrino+ has one transmitter and four beam receivers (see Figure 7). For three dimensional velocity measurements three beam receivers are adequate but the Vectrino+ consists of four because it records two independent z-velocities. There are different types of this Vectrino available: the down-looking probe, the side-looking probe and the field probe. For each type there is a version with a fixed stem probe and a cable probe. The Vectrino used for the measurements in the laboratory is a fixed stem side-looking probe (see Figure 7). The reason is that there are shallow waters in the model and that will be a problem for the down-looking probe. Also the fixed probe is preferred because of shallow waters and the easier installation on existing instruments [5] [8].



Figure 7: Vectrino side-looking probe [6]

The drawings in Figure 8 show the detailed structure of the Nortek Vectrino+ with a fixed stem side-looking probe.

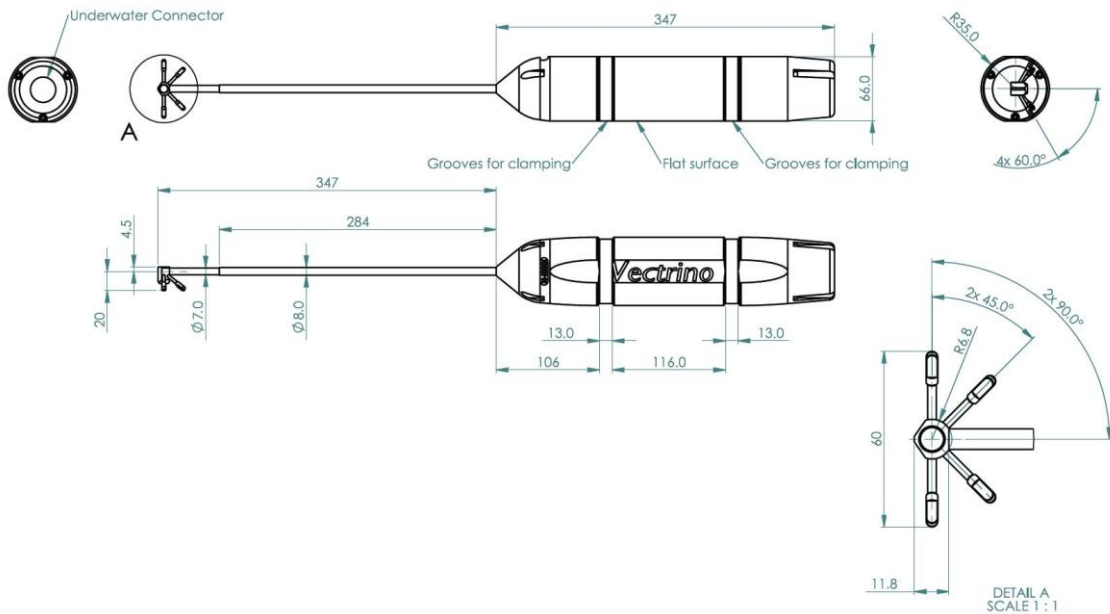


Figure 8: Datasheet Vectrino lab side-looking probe [16]

The Vectrino measures the velocities in three dimensions; this means there is one velocity component in x-direction, one in y-direction and one in z-direction. Figure 9 illustrates the positive coordinate system of the Vectrino. The positive z-directions faces upwards, the positive y-direction faces in the emitting direction of the transmitter and the x-directions is indicated with a red rubber band and normally shows in flow direction. The highest velocities should not be in the direction of the transmitter, best data is achieved if the main flow direction is perpendicular to the transmitting direction [15].

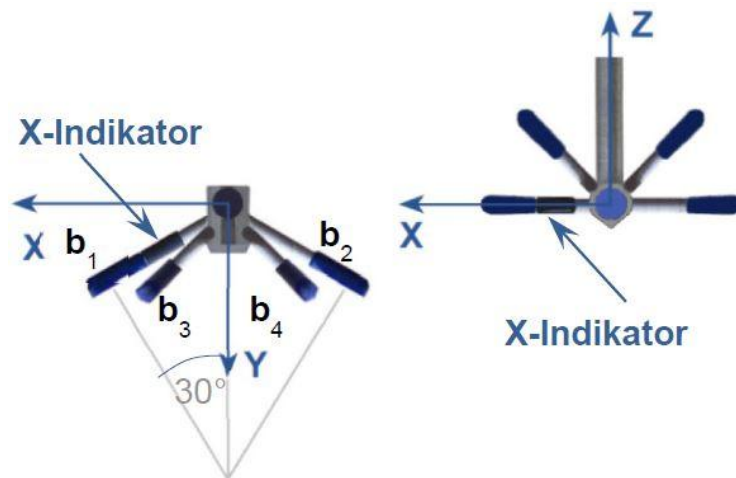


Figure 9: Vectrino side-looking probe indicator [17]

The Vectrino consists of a central 6 mm ceramic transmitter which transmits at 10 MHz and four ceramic receivers (6 x 3 mm). Figure 10 displays a Vectrino down-looking probe with a central transmitter and four receivers [7].

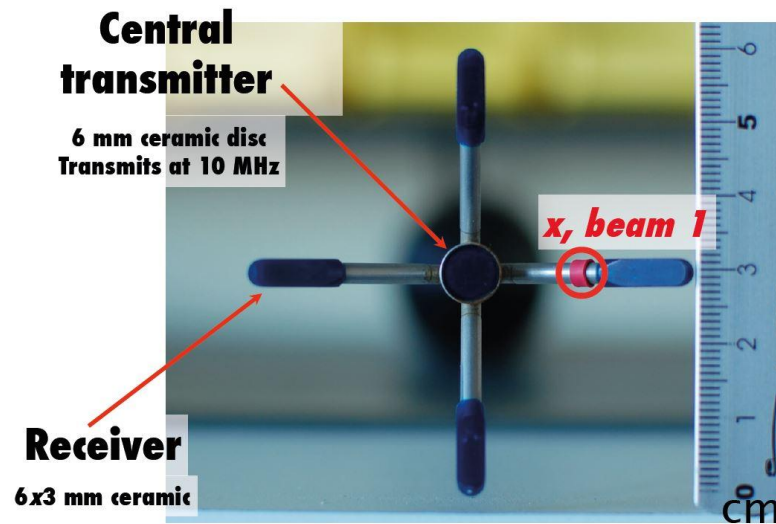


Figure 10: Vectrino components [7]

2. General

Before setting up the measurement in the model Gratkorn a comprehensive literature research on Vectrino measurements and post-processing is done. Moreover a test measurement is carried out in a laboratory flume to detect uncertainties and test the proposed solutions (chapter 3). This chapter is splitted in two parts, ADV-Measurement and WinADV Post-Processing.

2.1 Operating principle of the Acoustic - Doppler - Velocimeter

Acoustic Doppler Velocimeters operate with the principle of the Doppler shift effect which means that there must be relative motion between the source of sound waves and the observer. The shift in frequency can be calculated with the following formula [10]:

$$F_{doppler} = -F_{source} \frac{V}{C} \quad (1)$$

In this formula $F_{doppler}$ is the change in received frequency, the Doppler shift, and F_{source} is the frequency of the emitted sound waves. V is the velocity of the source of sound waves relative to the velocity of the observer and C is the velocity of the sound waves (=speed of sound). The ADV device emits acoustic waves into the water and these waves are reflected by suspended particles in the water. The reflected waves then are received by the four receiving beams. The probe determines the change of frequency in the reflected sound waves [10].

The Nortek ADV system is a bi-static (transmitter and receiver are separated) measurement system that collects simultaneously four values with each sample. These four values are a **velocity** component, a **signal strength** value (amplitude), the **signal-to-noise-ratio** (SNR) and a **correlation** value [5] [14].

The **velocity** component output is either in xyz-coordinates or in beam system coordinates; however, the transformation from beam to Cartesian (or trigonometric) coordinate system may cause some velocity resolution problems. The actual measured velocity is along the angle bisector between the transmitter and receiver as shown in Figure 11 [5] [14].



Figure 11: Vector v [14]

The **sampling rate** can be set by the user. With the Vectrino+ a sampling rate up to 200 Hz is possible (200 measured values per second are saved). The actual internal measuring frequency of the ADV, the so called ping rate, is not user-adjustable but it also changes if the sampling rate is amended. The ADV sends out pings into the water and then listens to the reflections of moving scattering material in the water. It is expected to be one ping in the sample volume at each time and the basic operation is ping-listen-ping-listen. The pulse repetition rate (PRT), the time between transmission of pulse 1 and pulse 2, describes this operation. The change in phase between pulse 1 and pulse 2 is used to calculate the velocity of scattering material in the sampling volume. The final velocity is an average of many velocity estimates (pings). This method produces high resolution and low noise data. The PRT cannot be set arbitrary small and there is a maximum range for the pulses. Nevertheless the user can change the PRT with the settings of the nominal velocity range [13] [14] [15] [17].

The **Nominal velocity range** describes the maximum velocity the device is able to measure. It is user-adjustable and should be aligned with the extremes of the flow velocities and the distance to the water surface. The nominal velocity range should be set as low as possible but slightly higher than the maximum expected velocity. This is done to minimize measurement uncertainty and noise. When it is set too low and the velocities exceed the nominal velocity range the measured values may become unusable or wrong. It has to be said that the higher the nominal velocity range the higher is the uncertainty in the measurement since there is more noise in the data. To get the optimum nominal velocity range a test measurement with a very high nominal velocity range should be done to determine the highest and lowest velocities. Then the nominal velocity range can be adjusted to these maximum and minimum values. Turbulence measurements may require a higher nominal velocity range otherwise the correlation values would be too low for post-processing. To achieve good data setting the velocity range appropriately is one of the most important steps the user has to do [13] [14] [15] [17].

The **amplitude** describes the strength of the return signal in digital counts. The amplitude expressed relative to the instrument noise level in dB is the **signal-to-noise-ratio**. The higher this value the better is the measurement. A good result is reached when the SNR-value is higher than 15, ideally higher than 20. As shown in Figure 12 the maximal SNR is reached at a distance of 5 cm from the transmitter [14] [17].

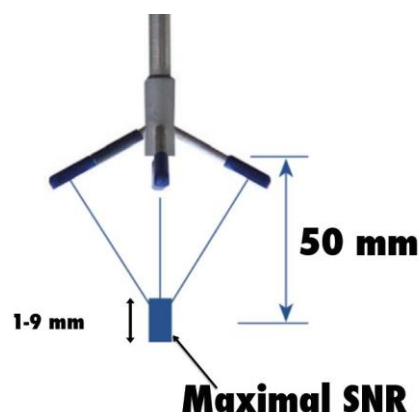


Figure 12: Maximal SNR [7]

For geometric reasons the sampling volume is around 5 cm away from the transmitter. Figure 13 shows the area which is covered by the four beams and the distances to the transmitter. Because of the geometric design no measurements in an area from 0-4 cm are possible and the best results are achieved in the so called sweet spot.

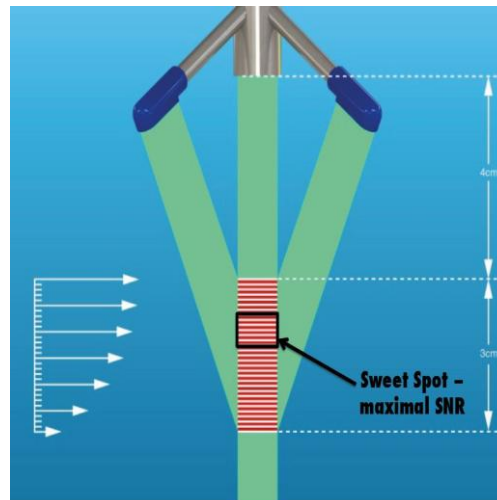


Figure 13: Vectrino Sweet Spot [7]

The **correlation** value describes the signal quality in percent and is the most important quality criterion for the measurement. The signal quality is defined by the similarity of two reflected pulses. 100 per cent would be the ideal correlation but values around 70 are described as good enough for measuring mean velocities. For more precise measurements (e.g. instantaneous velocities, turbulences) correlation values above at least 80 should be reached, preferably values between 90 and 100. Low correlation values can happen if the change of velocity is very high, if there is too little scattering material in the water or if there are some interfering signals [14] [17].

2.1.1 Configurations

In order to achieve good data the Vectrino+ software allows the user to set up a wide range of different settings for the measurement. Figure 14 shows the control panel of the Vectrino+ software. Normally the velocities in x-, y- and z- directions are displayed graphically; however, the operator can switch to displays of amplitude, SNR or correlation if needed. The velocities are also shown in numbers and also the main parameters of a measurement like standard deviation, amplitude, SNR and correlation can be read off the display. The side looking probe does not have a second measurement for the z-direction; the second value is outputted as zero. Another specification of the side-looking probe is that it can measure 2D-velocities near to the water surface because only the lower two beams have to be submerged to receive the x- and y-velocity. When the two upper beams reach out of the water a disturbed z-velocity will be recorded.

In Figure 14 the control panel with an accurate measurement is evident (correlation > 90, SNR ~ 15).

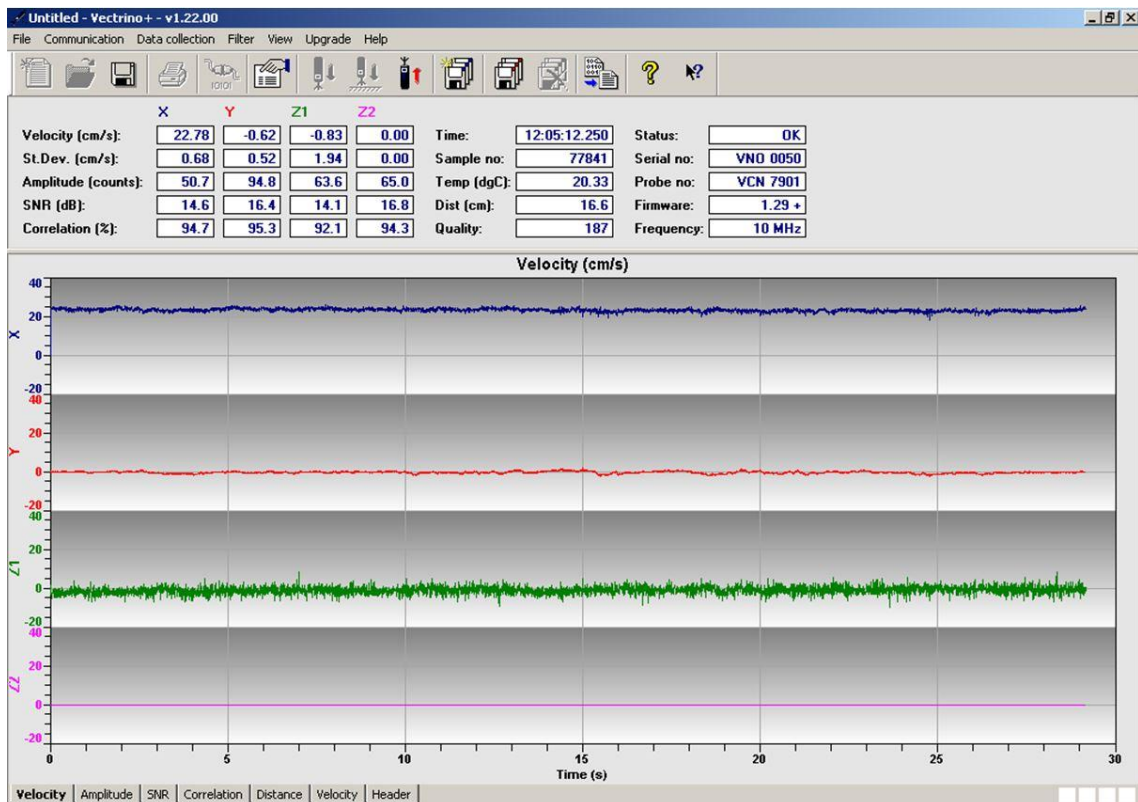


Figure 14: Control panel – accurate measurement

Furthermore, the time, the sample number and the measured temperature of the water is displayed. Another feature of the Vectrino is distance measurement and one distance measurement is done automatically before the velocity measurement starts. The quality value expresses the quality of the boundary distance measurement and the higher the number the better is the measurement (0 if not detected). On the very right side (see Figure 14) some bars about the Vectrino are apparent, for example the status of the device, the serial number, probe number and firmware. The last bar displays the acoustic frequency of the pings which are sent out of the central transmitter and this frequency is always at 10 MHz [12].

The first step before every measurement is to check the connection between the computer-software and the Vectrino device. This can be done with the “Check communication” bar in the tool bar area. The second step must be the set up of the configurations for the measurement.

In the configuration panel (see Figure 15) the main settings for the measurement are done. The settings which are presented in Figure 15 are the settings which were used most of the time for the measurements in the flume and in the model Gratkorn. Just in some specific areas the settings had to be changed slightly.

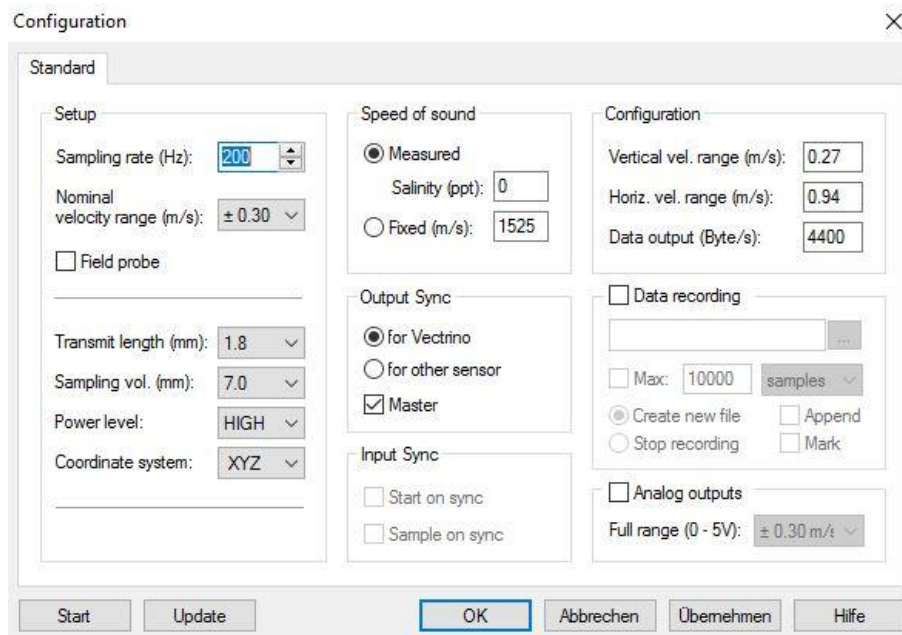


Figure 15: Configuration panel

The **sampling rate** should be set to highest possible value, in the Vectrino+ software this is 200 Hz. In fact this output rate means 200 values per second will be recorded. The more values are recorded the more accurate is the calculated velocity [12] [13].

One of the most important settings is the **nominal velocity range**. The available values are ± 0.03 m/s, ± 0.1 m/s, ± 0.3 m/s, ± 1.0 m/s, ± 2.5 m/s and ± 4.0 m/s. The nominal velocity range should cover all occurring velocities and the optimal range is descended before in a test measurement with a high nominal velocity range. The higher the nominal velocity range the more noise is in the data and vice versa [12] [13].

In the second part of the configurations the **transmit length** and the **sampling volume** can be changed. With the transmit length the volume of the sampling can be changed, the smaller the sampling volume the closer the measurement can get to boundaries or walls. It works the same the other way round, the higher the transmit length the bigger is the sampling volume. Possible settings are 0.3 mm, 0.6 mm, 1.2 mm, 1.8 mm and 2.4 mm. If the transmit length is changed the possible settings of the sampling volume will also change. Increasing the transmit length will lead to higher signal to noise ratios. Reducing the sampling volume will reduce the measurement accuracy because there will be less samples used for the velocity calculation [12] [13].

The **power level** describes the amount of acoustic energy which is transmitted into the water from the Vectrino. It should always be set to HIGH to receive the most accurate data [12] [13].

The last thing on the left side of the configuration panel is the selection of the **coordinate system**. Beam coordinate system or a fixed orthogonal xyz system can be selected. The beam system is in the coordinate system of the acoustic beams, about 15 degrees with respect to the vertical. For all the measurements the xyz coordinate system are selected [12] [13].

As described above the most important value for the quality of the velocity measurement is the **correlation** value. Figure 16 shows the correlation for an accurate measurement. The values are above 90 most of the time and there are just a few spikes downwards. Most of this data will remain after post-processing.

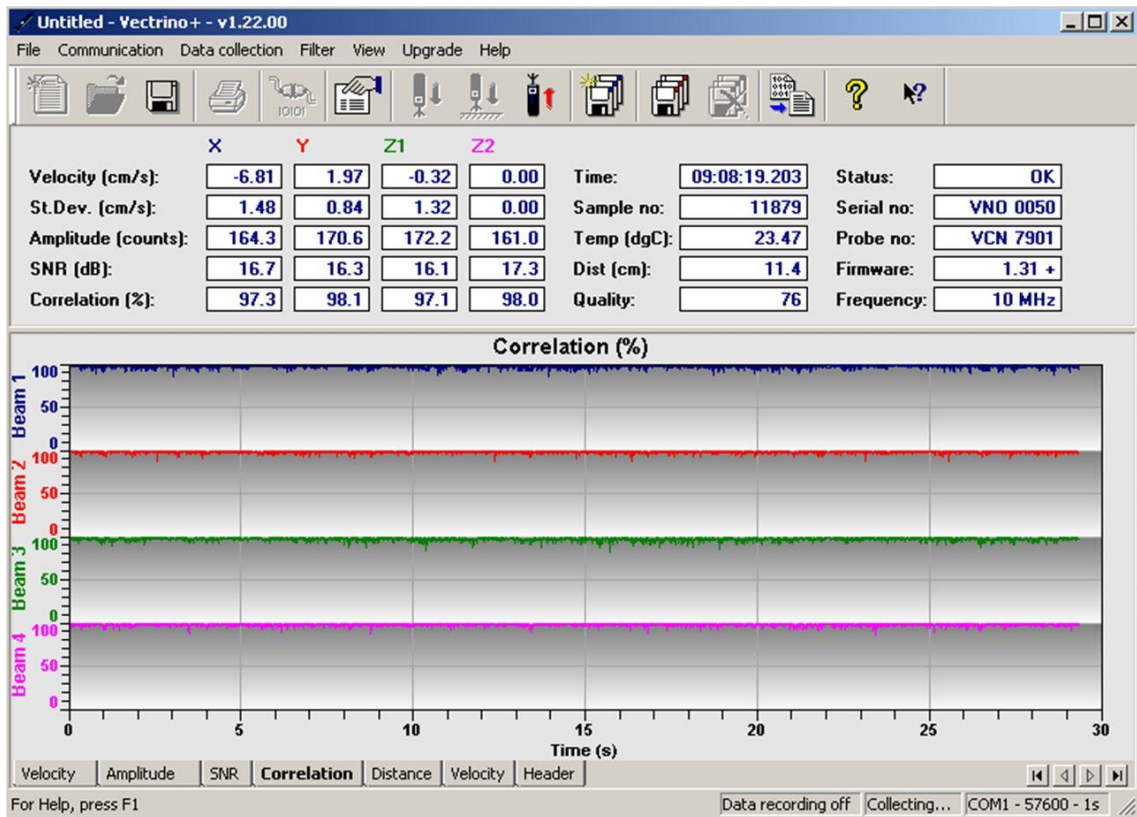


Figure 16: Correlation very high

For comparison a measurement with average correlation value just above 80 and SNR values lower than 10 is shown in Figure 17. The course of the correlation graph has an irregular form and a lot of spikes downwards. After post-processing less than 70 per cent of the recorded data remain.

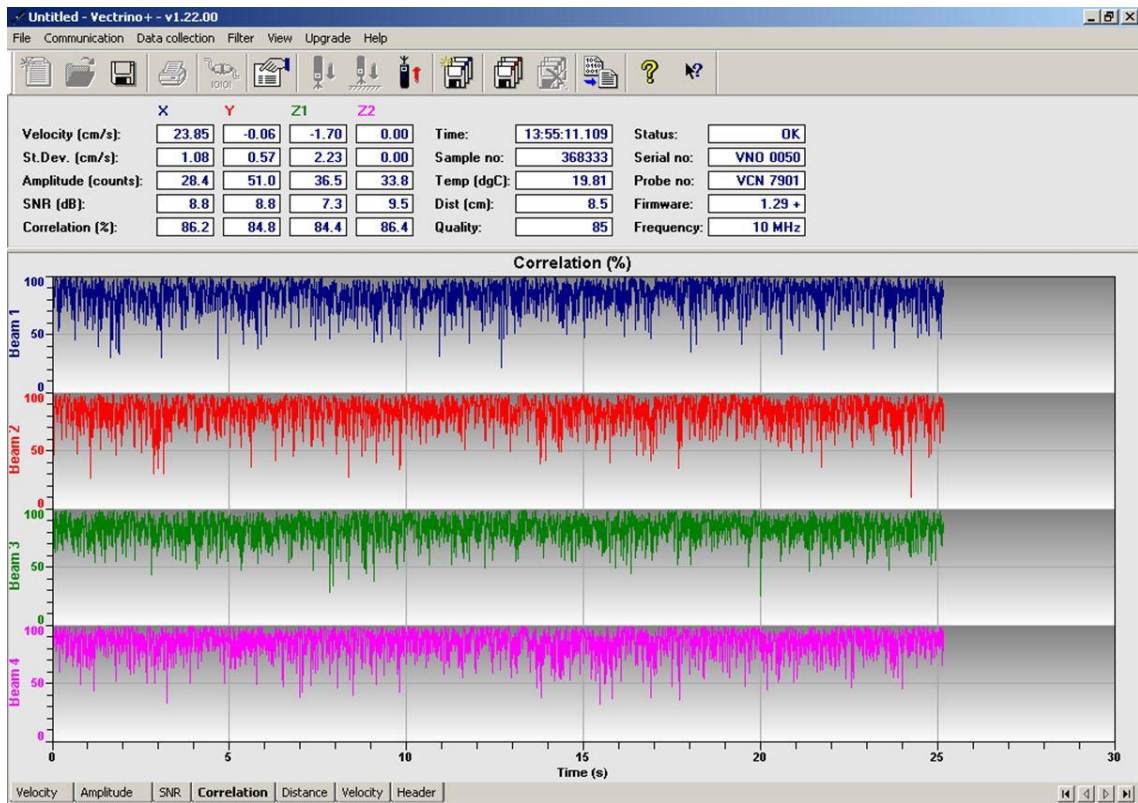


Figure 17: Correlation not high enough

Figure 18 shows an even worse measurement with correlation values below 80 and SNR values below 10. The velocity graphs have lots of ups and downs and in addition many upward and downward spikes. Also the standard deviation is very high (around seven centimetres per second). This measurement is unusable for further usage.

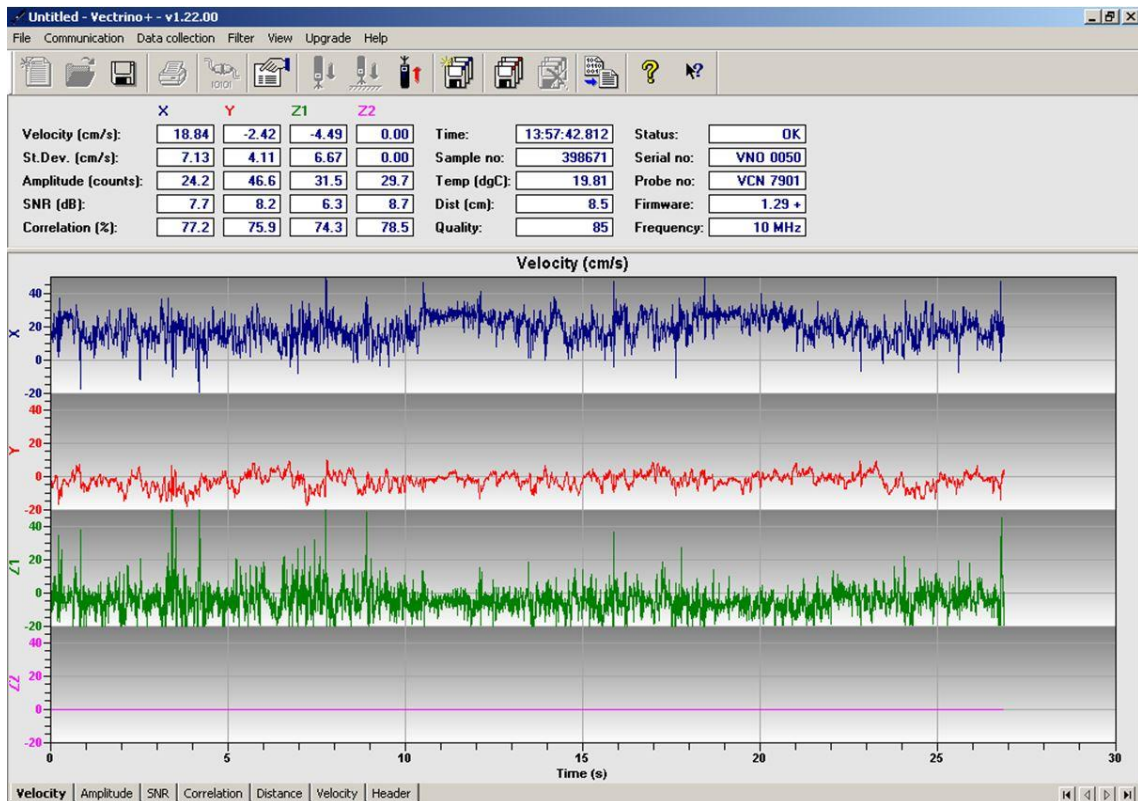


Figure 18: Inaccurate measurement

No matter how good the measurement is, the recorded data of the Vectrino always needs to be post-processed. In this case the post-processing was done with the free software WinADV and this procedure is described in chapter 2.2.

2.1.2 Troubleshooting

According to the Vectrino Guide [13] and Vectrino Quick Guide [15] there are five different reasons for noisy data:

- *Not enough particles in the water*
- *The velocity range being set too high*
- *The sampling volume being located beyond the bottom / wall*
- *Reflection and reverberation conditions at the bottom / wall*
- *Probe malfunction*

The first three problems are quite easy to identify and correct. If there are not enough particles in the water, the distribution of the particles will be inhomogeneous and will lead to low correlation and SNR values regardless of the position of the Vectrino. An easy solution is to add particles to the water (seeding) or increase the sampling volume. Another possibility is to enhance the transmit length or power level if it is not already set to the highest level.

A too high nominal velocity range will also lead to noisy data and wrong velocities. To get the optimal nominal velocity range a test measurement with a high nominal velocity range should be done to identify the highest occurring velocities. Then the nominal velocity range should be set slightly higher than the maximum velocity expected. So this problem is just a user-induced problem by choosing the wrong setting.

If the sampling volume is located beyond the bottom (down-looking probe) or beyond the wall (side-looking probe) no accurate velocities can be measured because there is too much noise in the recorded data. It is possible that the sampling volume is located in the bottom or the wall because it is located 5 cm away from the central transmitter. To solve this problem the position of the probe has to be modified to increase the distance to boundaries.

Another possibility of noisy data is the reflection of the transmitted signal from solid surfaces behind the particles in the water. Some of the acoustic waves are

reflected by the particles but the rest of the signal leaves the sampling volume and gets reflected by the bottom or walls behind the sampling volume. Also the water surface can reflect the passing sound waves. These reflected waves reach the sampling volume a second time and if this happens simultaneously with the incoming waves of the next pulse the measurement will be disturbed. So the echoes from past pings can affect the current measurement [14] [17].

Figure 19 illustrates a functioning measurement where the pings are sent out (e.g. at a sampling rate of 200 Hz) and the reflections are recorded and processed to an appropriate result (ensemble).

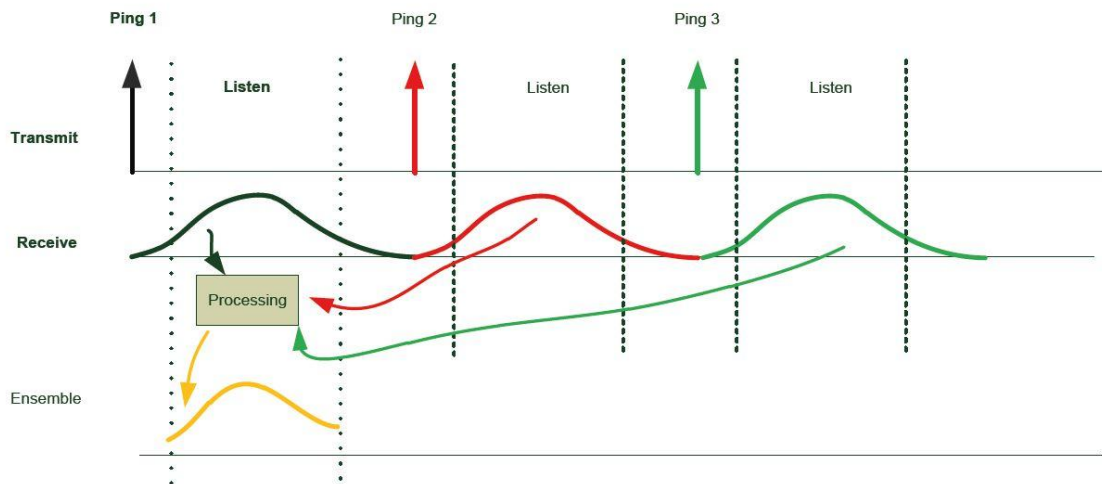


Figure 19: No Acoustic Interference [14]

If parts of Ping 1 get reflected by a solid surface behind the sampling volume and reach the sampling volume again simultaneously with Ping 2 an acoustic interference will occur. Figure 20 illustrates this acoustic interference problem.

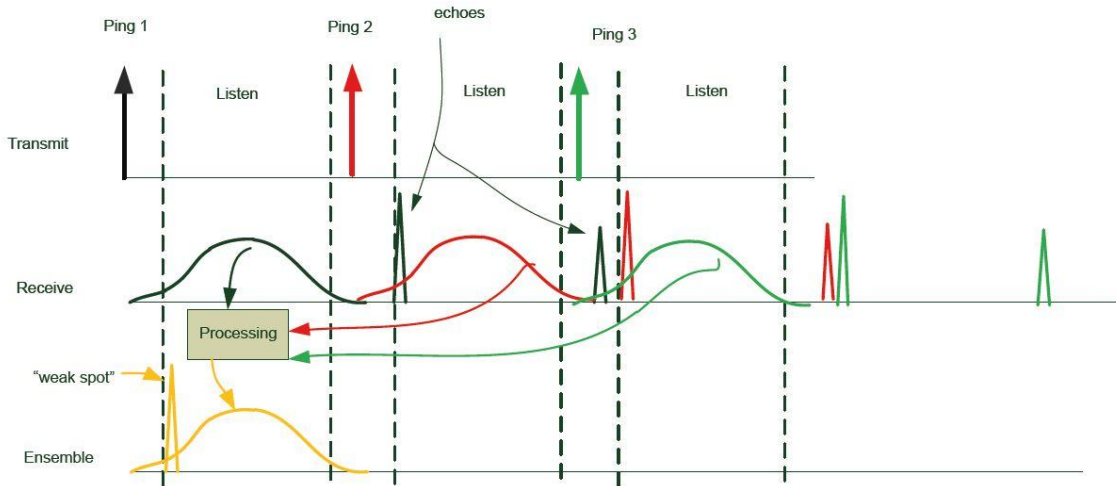


Figure 20: Acoustic Interference [14]

This can also be seen easily in the VECTRINO software. As shown in Figure 21 there is no possibility of an accurate measurement if the echoes influence the measurement. Even though the correlation and SNR values are high enough for an accurate result the measurement outcome cannot be used.

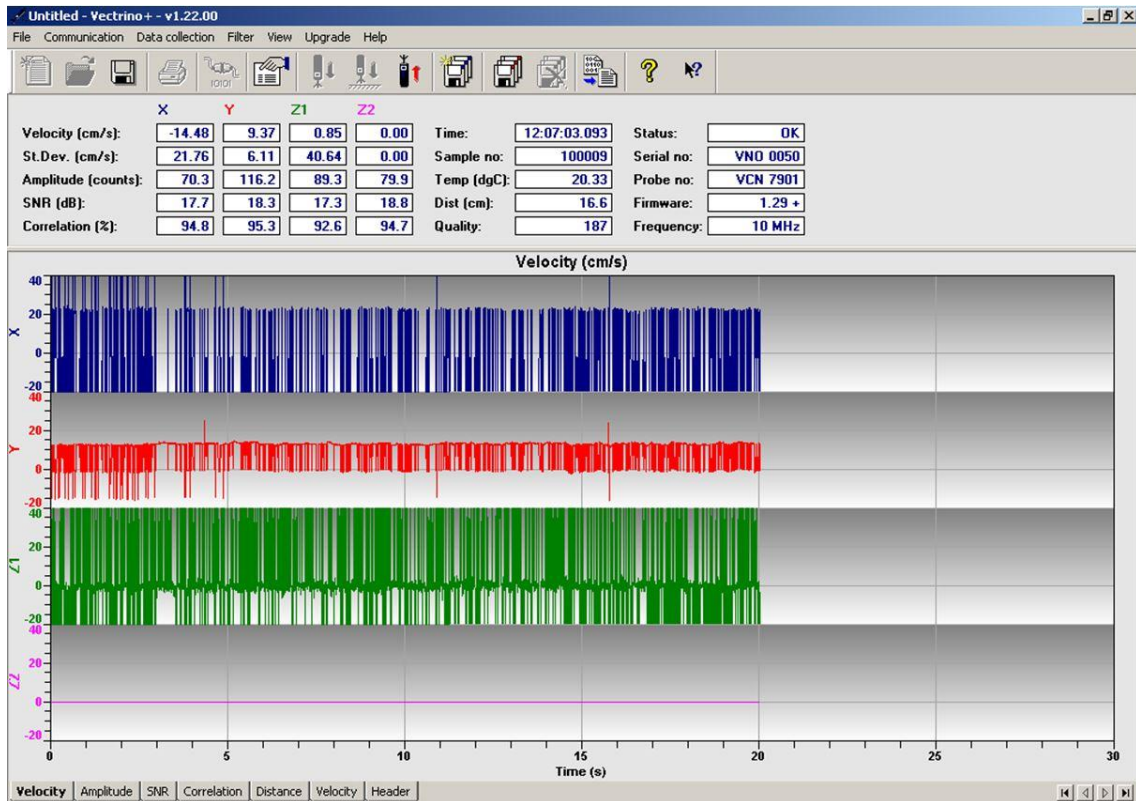


Figure 21: Interference problem

The one and only solution to this problem is to adjust the nominal velocity range because it has significant influence on the pulse repetition rate (PRT). If the distance between the pulses is longer than the boundary distance the acoustic interference problem is solved as shown in Figure 22 [14].

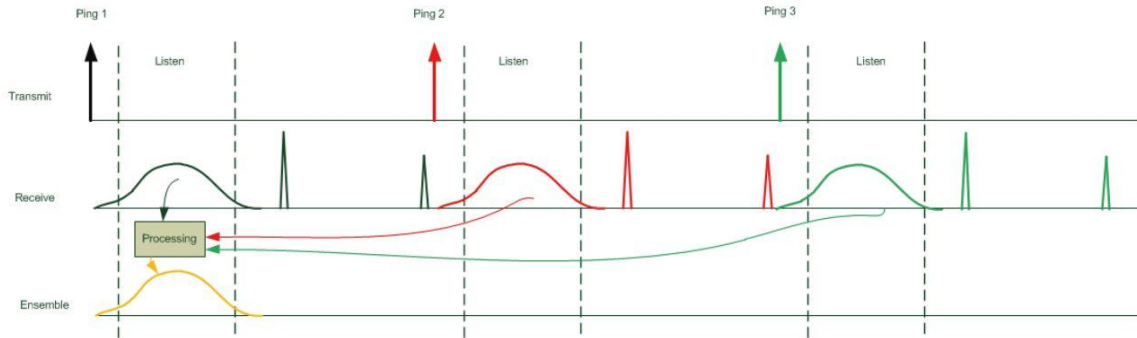


Figure 22: Solution of Acoustic Interference Problem [14]

Hence the distance from two pulses depends only on the nominal velocity range there are just a few critical distances where such disturbances can occur. For each nominal velocity range two critical distances exist. The first one results in the temporal difference of the first and second pulse. The second one results in the temporal difference to the next pair of pulses. These disturbances occur in areas ± 0.5 cm of these distances and they are called “Weak Spots”. The critical distances for each nominal velocity range are present in Table 1. To eliminate these malfunctions the nominal velocity range has to be set higher [17].

Table 1: Critical distances to solid surfaces [17]

Nominal Velocity Range	Critical distance from measuring volume centre to surface
$\pm 4,00$ m/s	2 cm and 5 cm
$\pm 2,50$ m/s	3 cm and 10 cm
$\pm 1,00$ m/s	5 cm and 12 cm
$\pm 0,30$ m/s	10 cm and 23 cm
$\pm 0,10$ m/s	23 cm and 45 cm
$\pm 0,03$ m/s	38 cm and 75 cm

These critical distances in Table 1 only account for solid smooth surfaces and if the transmitter axis is perpendicular to such a surface. Other boundaries like a

gravel bottom or structured/curved walls reflect the signal differently. In such cases the distance of the reflection has to be determined and these distances are not allowed to correspond with the critical distances from Table 1. These distances can be determined with the feature “Probe Check”. Figure 23 shows the result of such a probe check [17].

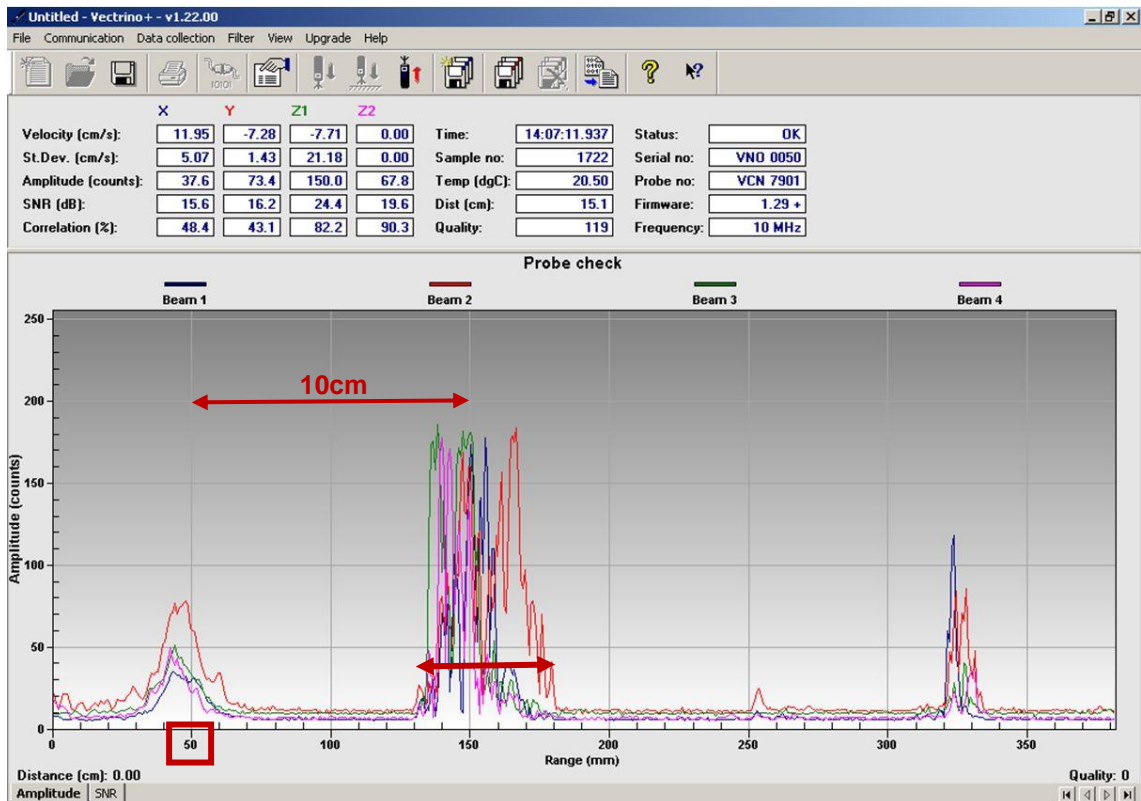


Figure 23: Probe check

In this graph the transmitter is at range 0 mm, the centre of the sampling volume is at range 50 mm and there is a reflecting area at range 130-180 mm (80-130 mm from sampling volume). The critical distance for a nominal velocity range of 0.30 m/s is 10 cm (see Table 1) and in this example reflections from a distance of 10 cm are received, so this measurement will be disturbed.

For measurements in high turbulence areas there is a further problem. If high turbulences occur the flow velocity fluctuates at a high rate and so the velocity

conditions in the sampling volume change between pulse 1 and pulse 2. Hence the two pulses are not similar any more, as a result the correlation values drop and the uncertainty of the correct velocity increases. A higher nominal velocity range can be a solution to this problem because the temporal difference of the two pulses is smaller with a higher velocity range. In fact the uncertainty of the single measured values gets higher but normally the mean values do not change significantly. Other solutions with turbulence measurements can be seeding (adding particles into the water) or changing the transmit length which also changes the temporal difference between the two pulses [17].

For high turbulence measurements a suitable post-processing technique is of very high importance. *Chanson, H., Trevethan, M., & Aoki, S. I. (2008)* [see 18] proposed further steps of detailed post-processing techniques to achieve the best data out of turbulence measurements. *Cea, L., Puertas, J., & Pena, L. (2007)* [see 19] also worked on this turbulence problem and compared four different filters for post-processing: a maximum/minimum threshold, an acceleration threshold, a phase-space threshold and a new filter. At areas with low turbulence all four filters worked quite well and delivered similar results. However in areas with very high turbulences none of them were able to distinguish between valid and corrupted data. *Castillo, L. G., & Carrillo, J. M. (2014)* [see 20] also tried to get accurate data out of turbulence measurements and they also compared the methods described above. There are several studies available on this turbulence problem, however a general solution is not available [18] [19] [20].

In this work the turbulences at the model Gratkorn are not expected as very high and so the post-processing with WinADV expected to deliver satisfying results. If the correlation and SNR values are too low seeding can be added to the stream and the measurement quality will increase immediately.

2.2 WinADV-Post-Processing

As already mentioned the recorded data from the Vectrino measurement cannot be used without proper post-processing. The quality of each single measurement has to be checked and, for the ADV typical, spikes have to be removed. There are many post-processing software products with similar functions available like ExploreV from Nortek and WinADV from the U.S. Department of Interior, Bureau of Reclamation, Water Resources Research Laboratory. WinADV is a common and free software since 1996. In this study it is used for the post-processing of the recorded data from the flume and the model Gratkorn [17].

During the measurement the Vectrino software records the data and saves it as a **vno-file**. This file contains, accordingly to the adjusted sampling rate, the time series of the velocity components in x- and y-direction, the two independent time series of the velocity component in z-direction (z1 and z2) and also the amplitude-, SNR- and correlation values. For the post-processing with WinADV these vno-files have to be converted to **adv-files**. There is a Data Conversion Tool in the Vectrino software and to get adv-files the NDV button in the options section has to be selected. The files should have the coordinates of the measured point in the file name so later the files can be identified and matched with their right position. After importing the adv-files into the WinADV software, the time series of the velocities, signal amplitude, SNR- and correlation values are displayed. Also the histograms (distribution of velocity and signal quality data) and the power spectrum for each of these values can be analysed. On the bases of these graphs, a rough estimation of the quality of the measurement can be done. A measurement with a high quality is characterized by high SNR- and correlation values and a constant velocity with few spikes. Figure 24 illustrates the WinADV interface and such a high quality measurement where more than 90 per cent of the data can be used after the post-processing procedure [17].

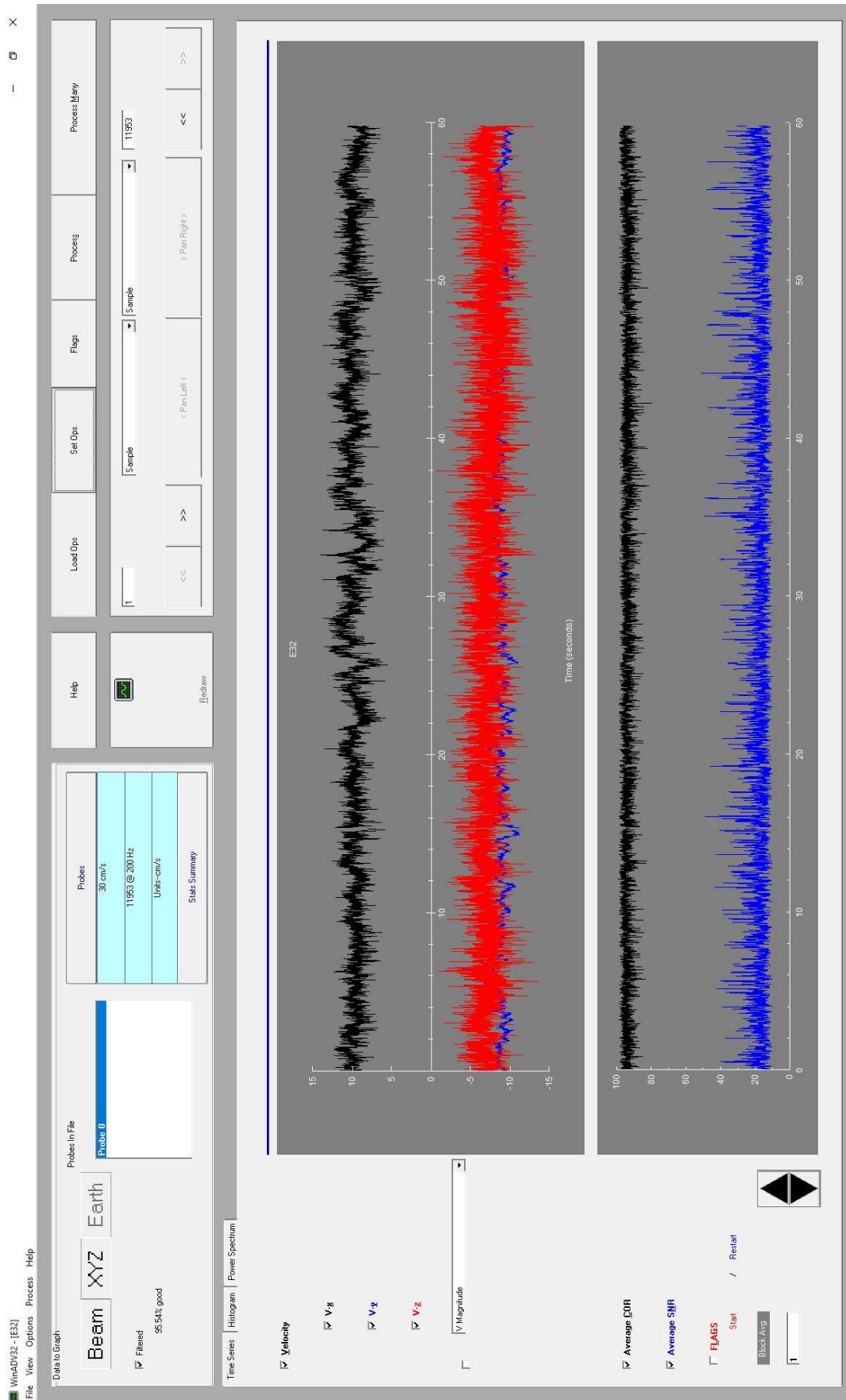


Figure 24: Control panel WinADV software

In the filtering options panel eight different filters can be selected. The first available option is the **correlation filter** option. Correlation values below a certain limit are removed. This limit can be set for the average of all the three channels or for the lowest one of them. The average filter removes fewer values than the minimum filter but the uncertainty of the measurement is higher. A typical value for the correlation filter would be 70, so all measurements with a correlation lower than 70 will be removed. The same filtering can be done with the **signal to noise ratio filter**, also an average or a minimum limit is selectable. WinADV also allows data filtering in a specific **velocity range** which is user-selectable. Finally there are also two spike-filtering algorithms which first detect the spike and then replace or remove the spike. The **acceleration spike filter** removes a spike when the acceleration exceeds a specific threshold (normally 1–1.5). Otherwise the **Phase-space threshold despiking method** from *Goring & Nikora* [see 17, 22 and 23] works differently. It uses the concept of a phase-space plot in which the variable and its derivatives are plotted against each other. All of the points which are outside an ellipsoid defined by the Universal criteria are designated as spikes. This method iterates until the amount of good data remains constant. WinADV also filters out **communication errors** and they can be replaced with interpolated values. All these filtering options can be selected separately or in every desired combination. It has to be said that if one receiver delivers an incorrect value in a time step the data of all receivers at this time step will be removed. Furthermore, WinADV removes incorrect values or spikes and does not replace them. After the filtering the data can be exported to **ASCII files** which can be read by other software like Excel. Another useful advice is to indicate the amount of good data and the average correlation values additional to the results of the measured points for quality assurance [17] [22] [23] [24].

Figure 25 illustrates the selected filtering options for all of the measurements in the flume and also in the model Gratkorn. The correlation filter is set to 70, the SNR filter is set to 10 and the Phase-space threshold despiking filter is activated.

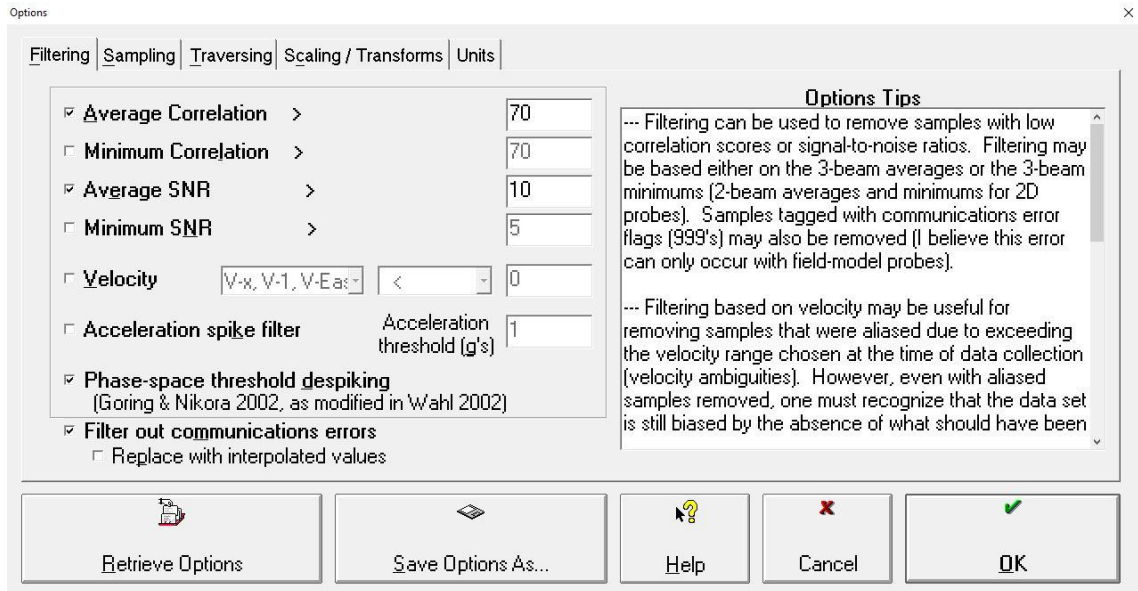


Figure 25: Options panel WinADV software

There are some other settings available in the options panel like which samples should be filtered (Sampling) and if there is a measurement with a traversing Vectrino (e.g. in a river). In the Scaling / Transforms window the scale for a Froude model can be added and the velocity will be calculated automatically to the reality. Also a plane rotation for all velocities can be done; this is very useful if the Vectrino probe has to be used in reverse near boundaries. In the window Units the user can decide which units should be used, the units of the measurement or the native units of each file.

When measuring near the bottom (3 – 5 cm) and in very turbulent areas the correlation values drop beyond 70 and so a lot of data has to be removed in the post-processing step. After post-processing often less than 70 per cent of good data is left. Measuring points with less than 70 per cent of good data should be removed completely and not used in further calculations. The most probable cause for problems in these areas is boundary interferences. *Martin, V. et al.* describe this low correlation problem near the bottom and in turbulence areas [see 21]. They found out that the correlation does not necessarily demonstrate the quality of the data. Especially because low correlation values do not bias the mean velocity of the measurements. In their experiments they came to the conclusion that correlation values of 30 are high enough for mean velocity measurements. In their measurements they used the 70 per cent correlation filter and kept the data where more than 70 per cent of data was good after post-processing. With the other points they used the 40 per cent correlation filter and also kept points with more than 70 per cent good data. The result was that the spike detection filter also delivered similar results like the 40 per cent correlation filter and that the filtering criterion can be as low as 40 per cent and also delivers accurate average velocities [21].

Figure 26 illustrates the comparison of different filters and data remained after post-processing. Near the bottom a lot of data is unfeasible due to reflections.

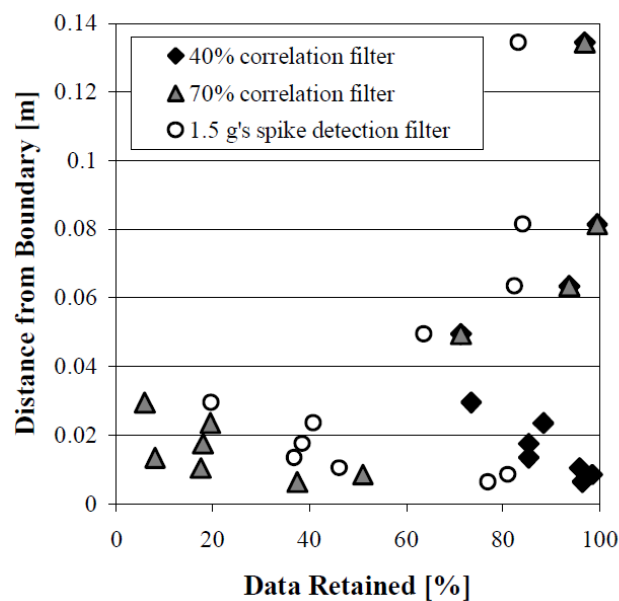


Figure 26: Correlation Filter [21]

2.3 Recapitulation

Based on the previous sections some important determinations regarding the ADV-measurements and the WinADV-post-processing are stated.

For the velocity measurements in the flume and the model Gratkorn the following settings for the Vectrino+ software are decided:

- Correlation values should be at least higher than 80, ideally between 90 and 100.
- SNR values should be at least higher than 10, ideally higher than 15.
- Standard deviation should be checked during measurements, should not be too high.
- Seeding from the bottom of the water tank can be added if the quality indicating values are too low.
- If the sampling volume is near the “Weak Spots” the measuring points can be shifted slightly.
- Sampling rate should be set to highest possible (200 Hz for Vectrino+).
- Nominal velocity range should be set slightly higher than the expected velocities. Most of the time it is 0.30 m/s or 0.10 m/s. If there are reflections or interferences it can be set to a higher value to deal with this problem.
- Transmit length is left at default value (1.8 mm).
- Sampling value is also left at default value (7.0 mm).
- Power level should be set to HIGH.
- Coordinate system is the xyz-coordinate system.

For the post-processing with WinADV the following settings are selected:

- The correlation filter is set to 70 on average.
- The SNR filter is set to 10 on average.
- The Phase-space threshold despiking method is activated.
- Communication errors should be filtered out by the software and not replaced with interpolated values.
- The plane rotation for the xy-plane should be set to 180 degrees if the Vectrino has to be reversed.
- Each file's native units are used.
- All measurement points are filtered with the same settings.

Furthermore, the discharge in the model Gratkorn is recorded to guarantee constant discharge and subsequently constant velocities.

3. ADV - Measurements in a laboratory flume

Before the measurements on the model Gratkorn are performed, it is necessary to test the functionality of the Vectrino. This is done in a laboratory flume in the laboratory. In this flume the measurements near the boundaries and other “Weak Spots” can be tested and improved. Also obtained data is used for testing the post-processing with WinADV.

3.1 Set-up of measurement

The flume is 20 cm wide and the water level is adjusted at 14 cm above the bottom so the depth is similar to the water depths expected in the model Gratkorn. Care was taken that steady-state and uniform flow exists during the measurement. A raster with the measuring points is created consisting out of 81 points. A cross section of the flume and the arrangement of the grid are shown in Figure 27.

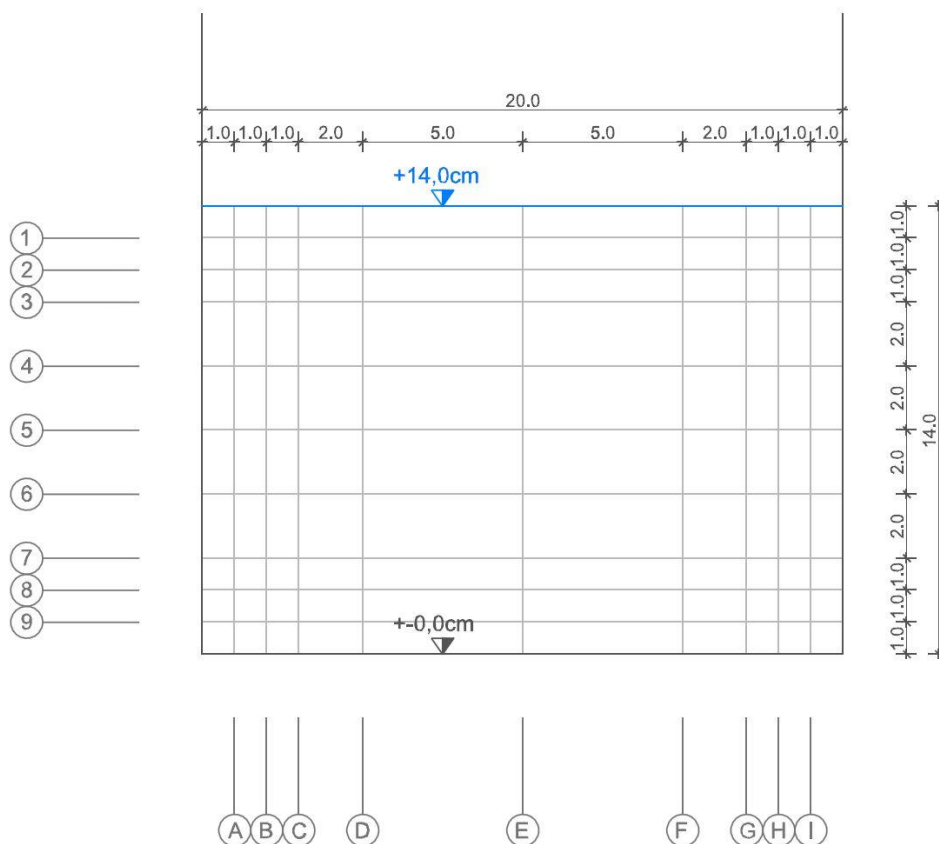


Figure 27: Raster glass channel

Special attention is given to the areas near the bottom, the walls and the surface. Therefore the grid in these areas is narrower to obtain information how close to these boundaries the measurement will still be accurate and the data useful. Near the boundaries (bottom, walls and surface) the distance between the measurement points is one centimetre – with the distance increasing towards the centre. One test series is also done 5 cm away from the boundaries to check the “Weak Spots” for the used nominal velocity range of 1.0 m/s. For this velocity range the critical distances to the boundaries are 5 cm and 12 cm (see Table 1).

Figures 28 and 29 show the installation of the Vectrino device in the glass channel. Height and width are easy adjustable, either automatically or by hand.



Figures 28 and 29: Installation of the Vectrino+

The measurement time for each point is set to two minutes, giving the software enough time steps to calculate the mean velocity. At a sampling rate of 200 Hz and a measurement time of 120 seconds there are around 24,000 single values for each parameter recorded. This has to be carried out because the needed measurement time for each point is not clearly stated in the literatures. The points in the flume are examined to find out at which timestep the mean velocities do not change anymore. This investigation is carried out to find the minimum amount of timesteps needed for the measurements in the model Gratkorn.

Figures 30 and 31 demonstrate the Vectrino probe submerged into the water. As described before, 2D measurements are also possible if the top two beams are not placed beneath the surface (see Figure 31). To measure the top row of the raster (1 cm below water surface), it is necessary to adjust the probe in a height where the top two beams reach out of the water. For this measurement row the z-velocities are disturbed but the x- and y-velocities are still accurate.

Problems with the quality parameters occur because the water in the laboratory is too clean and there are not enough particles in the water to reflect the sound waves. So sediments from the water tank are added as seeding.



Figures 30 and 31: Vectrino+ in application

3.2 Results

The recorded data is saved as vno- and vna-files and those have to be converted to adv-files in order to import them into WinADV for post-processing. After filtering the data with the earlier described options (chapter 2.2 and 2.3), the data is saved in ASCII-format which is readable by Microsoft Excel. Two files for each point; one summary file of the filtered data and one summary file of the unfiltered data, are compiled.

For each single point and time step the following parameters are recorded: the time, position, if there is a flag, velocities in x-, y- and z-direction, the correlation for each beam, the SNR for each beam, the amplitude for each beam and average values for correlation, SNR and amplitude (Time, Position, Flag, Vx_0, Vy_0, Vz_0, COR0_0, COR1_0, COR2_0, SNR0_0, SNR1_0, SNR2_0, AMP0_0, AMP1_0, AMP2_0, CORAvg_0, SNRAvg_0, AMPAvg_0).

The summary file of the filtered and unfiltered data contains the file name, the sample rate, velocity range, velocity scaling, coordinate system, probe number, boundary distance, sampling window, traverse options, time span, sample span, number of samples, number of good samples, per cent of good samples, filter options, units, average velocities in x-, y- and z-direction, magnitude of average velocity, average of velocity magnitude and average correlation, SNR and amplitude. Also several other data, not relevant to this thesis, is stored like skewness, kurtosis, covariance, temperature, pressure, salinity and conductivity.

For further usage these tables are modified and adjusted so that they can be read by a python code which displays velocity contour plots. Figures 32 and 33 show the results of the measurements in the flume as contour plots for velocities in x-direction and the magnitude of the average velocities:

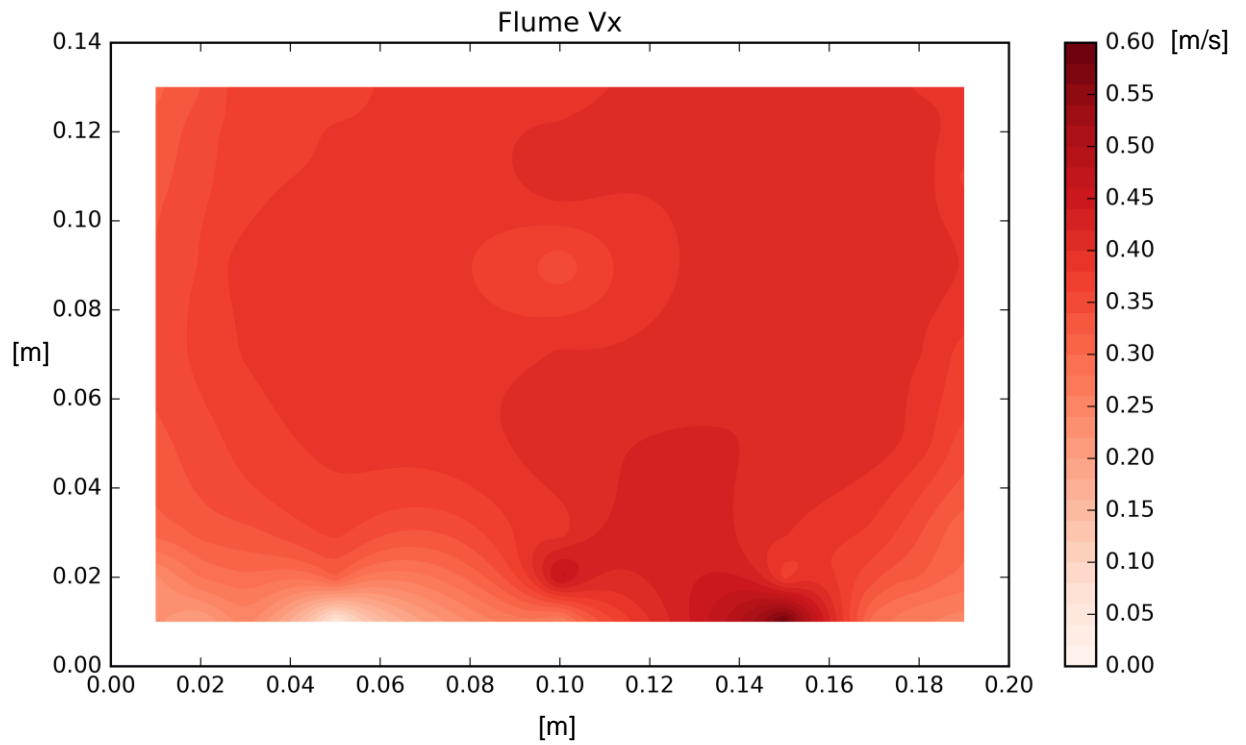


Figure 32: Velocities in x-direction in flume

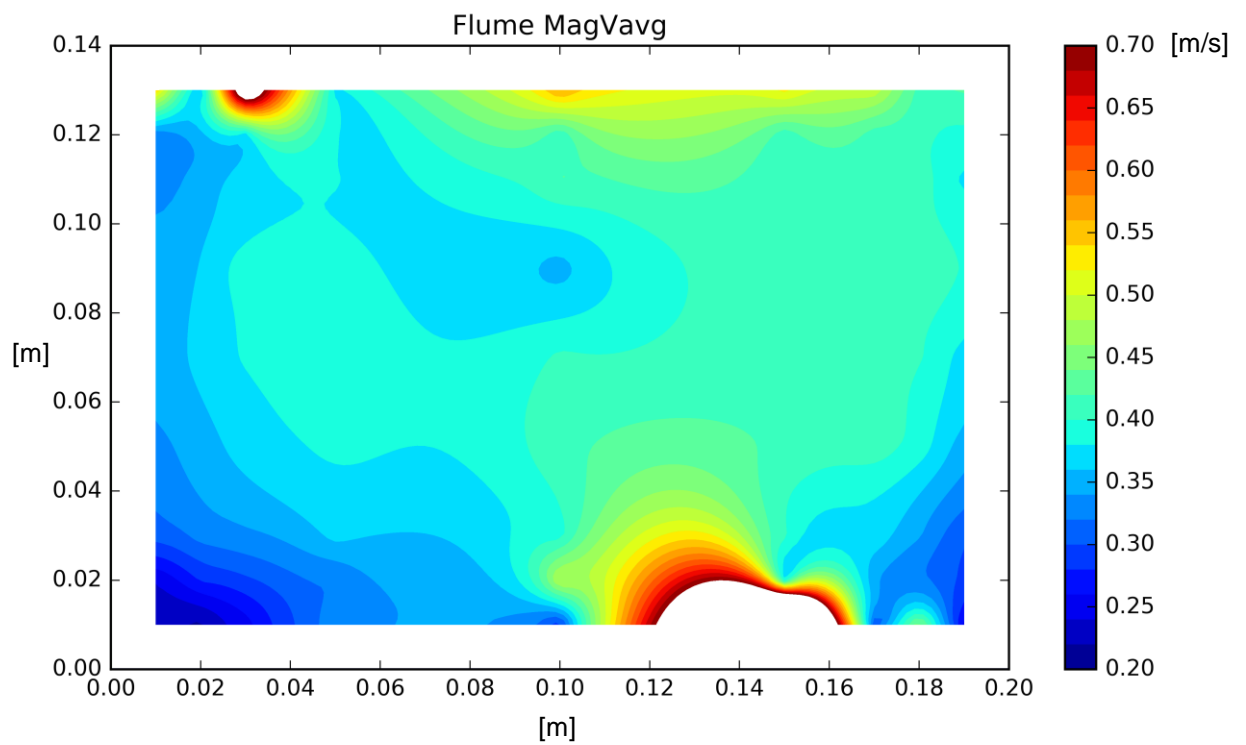


Figure 33: Magnitude of average velocities in flume

The velocities in the flume are nearly constant and evenly distributed reaching a maximum of about 0.60 m/s. These contour plots also show some serious problems in the area near the bottom caused by reflections and near the surface caused by the z-velocities because the two upper beams reach out of the water.

Now the criteria is applied that more than 70 per cent of good data has to be left after post-processing and the other points are erased. Figure 34 illustrates how much good data is left:

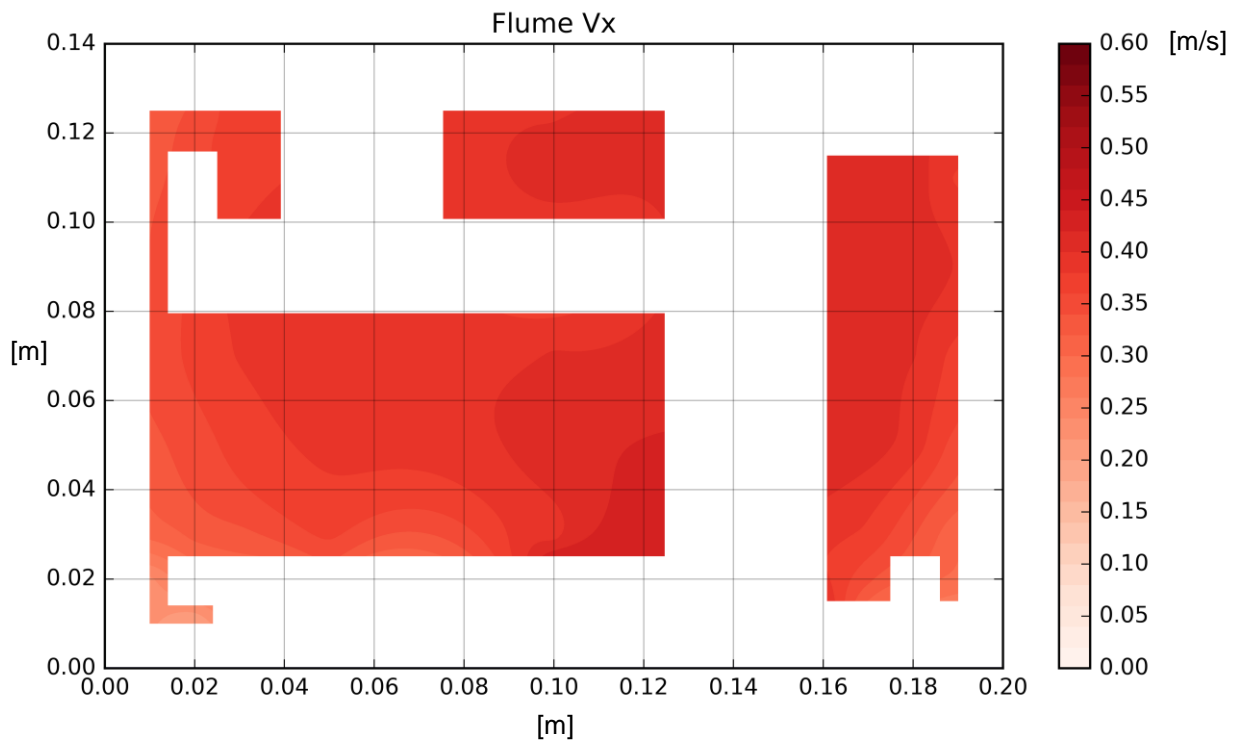


Figure 34: Velocities in x-direction in flume masked

This plot shows that there is an uncertainty in the first two centimetres near the bottom and in the measurement rows 5 cm away from the surface and walls (“Weak Spots”). This measurement clearly proves the interference problem described in chapter 2.

The reason for the white border around the contour plot is that the flume measures 20 cm in width and the water surface is 14 cm above the bottom but the first measurement points start 1 cm away from the boundaries. So there is no

available measured velocity between the boundaries and the first row of measurement points, therefore this area is left blank.

The next step is to find out how long a measurement should take. All 81 points in the flume are measured for 120 seconds at a rate of 200 Hz. For the calculation with python all the time steps are used to get a mean velocity (see Figure 35, red line). The blue line illustrates the course of formation of the mean value. At the beginning, the mean of the first two points is computed, then the mean of the first three points and so on until all 24,000 time steps are included in the calculation of the mean velocity. Therefore at the end the blue line and the red line unite in one point. The difference between the red and blue line shows how much discrepancy is at a specific time step between the final and the present mean velocity. Figure 35 illustrates exemplary for all 81 points how the course of such a graph looks like. In this case for point L4PH (see Figure 35) the final mean velocity is reached after about 60 seconds. The graphs for all the other points are attached at the end of the thesis.

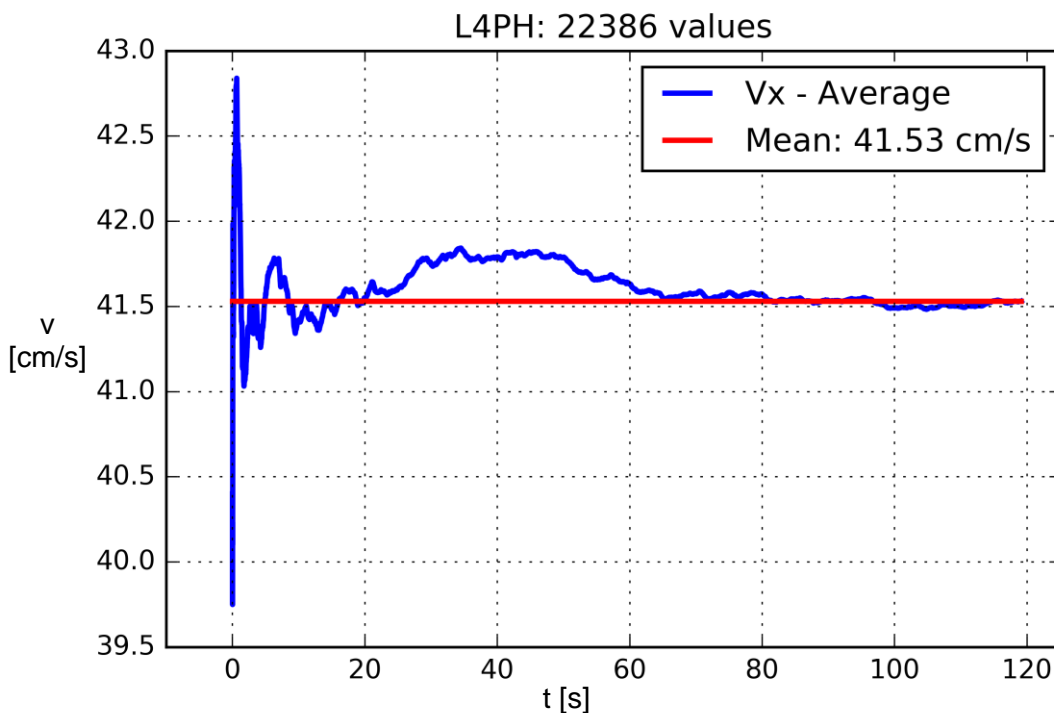


Figure 35: Point L4PH

This calculation is done for each of the 81 points and every point is considered individually. Table 2 shows the time elapsed at each point to reach the mean velocity.

Table 2: Measurement time for each point in the flume to get mean velocity

	A	B	C	D	E	F	G	H	I
1	20s	20s	40s	60s	20s	50s	30s	30s	40s
2	30s	30s	40s	30s	40s	30s	40s	30s	40s
3	50s	40s	20s	30s	40s	20s	20s	20s	30s
4	20s	40s	70s	30s	20s	40s	20s	30s	20s
5	30s	20s	20s	30s	30s	30s	20s	30s	20s
6	40s	40s	20s	30s	30s	60s	20s	20s	30s
7	20s	20s	40s	20s	40s	30s	20s	20s	30s
8	15s	40s	80s	80s	60s	30s	40s	30s	30s
9	40s	60s	30s	80s	100s	40s	10s	40s	70s

This analysis shows that for most of the points the mean velocity is reached after 40 – 60 seconds. In some cases near the boundaries the mean is obtained as late as after 80 –100 seconds. Points with more than 70 per cent remaining data after filtering reach their mean velocity in less than 60 seconds. For the other points there are just a few hundred time steps left and so the graph makes big jumps around the mean line. The calculation of all 81 points can be found in the appendix.

3.3 Improvement / Modification

The measurements in the laboratory flume show the importance of the probes location concerning the results. Near the boundaries the measurement can be inaccurate, especially close to the bottom. The plots illustrate that in an area of 1 – 2 cm near the bottom the correlation and SNR values drop and these points are then filtered out in the post-processing procedure. Also there is a huge problem with the z-velocities near the surface because of the top two beams reaching above the surface. These points are also filtered out. Near the walls there are no major discontinuities but the area of the “Weak Spots” must be taken into consideration. This means changing the settings of the Vectrino (e.g. nominal velocity range) to obtain accurate data. In short measurements very close to the bottom and the surface are difficult and that has to be considered for the measurements in the model Gratkorn. The best solution is to start the first row of points at a distance of 3 cm from the bottom and not getting closer than 2 cm to the surface. Also the distance to the walls should be at least 2 cm so inaccuracy in the measurements is prevented. If the measurement is in an area where reflections are problematic (e.g. “Weak Spots”) the settings of the Vectrino need to be adjusted until the measurement parameters improve.

The measurement time analysis (see Figure 35 and Table 2) indicates that a measuring time of 60 seconds is enough if the quality parameters are good enough. If measurement outliers occur the measurement at these points needs to be repeated. In case of the laboratory water being too clear for measurement seeding (e.g. sediments of the water tank) has to be added.

4. Laboratory Model Gratkorn

4.1 From hydropower plant Gratkorn to model Gratkorn

The hydropower plant Gratkorn is situated in the southeast of the town *Gratkorn* at the river *Mur* between the two already existing hydropower plants: *Weinzödl* and *Sappi* (see Figure 36). The storage level is at a height of 371.00 meter above the sea level, the downwater area is 1310 m long with a deepening of the downstream river bed by 3 m. The reservoir area is 3260 m long [11].

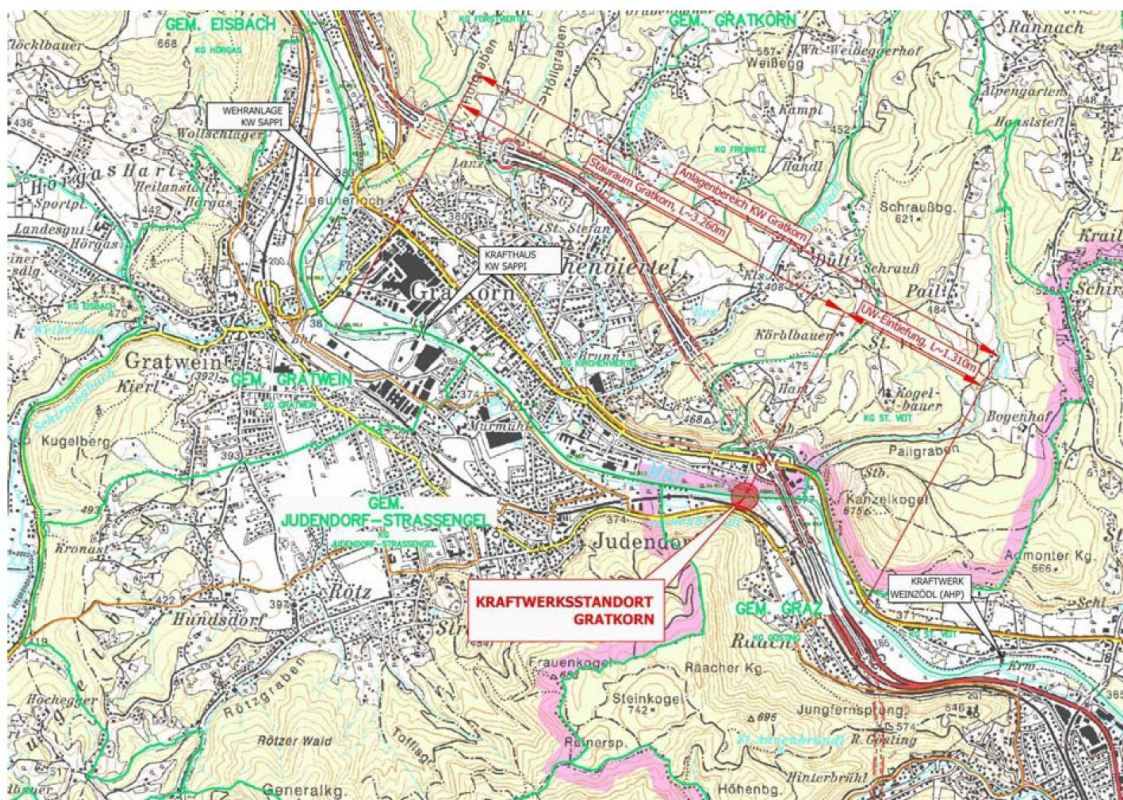


Figure 36: Location plan KW Gratkorn [11]

With a hydraulic head of 6.46 m and a discharge capacity of 205 m³/s the hydropower plant Gratkorn will have capacity of 10.8 MW and secured capacity of 2.9 MW. The hydropower plant consists of a powerhouse and a weir system. The powerhouse is on the right side of the river. Next to it there are three weirs, each 16.5 m wide with a radial gate and a superimposed flap gate. The energy dissipation happens in a straight stilling basin with a downstream sill. In the powerhouse there are two *Kaplan*-turbines with a discharge capacity of

102.5 m³/s each. The standard annual production is 52.7 GWh, which equals to the amount of electricity needed for the average supply of 13,200 households. In addition the net stability will be increased by this power plant. Compared to a coal-fired power station with the same capacity about 44,000 tons of CO₂ are saved each year. Furthermore, additional actions around the power plant are planned to increase the quality of life in the area for people, fauna and flora [11].

The hydropower plant Gratkorn is a project of VERBUND and ENERGIE Steiermark with an investment volume of about 70 mio €. The construction time is expected to be 26 months. The start of construction was planned in 2014 with a completion expected in 2017. Due to falling electricity prices the construction is postponed [11].

An exact model of the hydropower plant Gratkorn was built in the laboratory of the Institute of Hydraulic Engineering and Water Resources Management at the TU Graz in a *Froude* scale of 1:40 (see Figure 37). Froude's law describes the similarities between the model and the prototype with regard to geometric, kinematic and dynamic similarities. The Froude numbers of flow in the model and the nature are equal. It is a common similarity law for laboratory models with free surface flows and also common for fully turbulent pressurized pipes. In Froude's law viscous friction is neglected because in turbulent flows the apparent turbulent shear stress outweighs the viscous friction. Inertial forces and gravity play a role in this law because they are dominant. If the inertial force and the gravity work simultaneously then they are equal ($M_{FT} = M_{FG}$) resulting an equal acceleration of gravity in the nature and the model ($M_g = 1$) [25].

$$M_l * M_t^{-2} = 1 \quad (2)$$

For the time scale, velocity and discharge the following formulas apply [25]:

$$M_t = M_l^{1/2} \quad (3)$$

$$M_v = M_l * M_t^{-1} = M_l^{1/2} \quad (4)$$

$$M_Q = M_l^3 * M_t^{-1} = M_l^{5/2} \quad (5)$$

As shown in Figure 37 there is a straight flow to the structural barrier with dams on the left and right waterside. Then there are the three weir fields and on the right side there is the powerhouse with two turbines. The approach flow to the turbines is of high importance so that the turbines can work with high efficiency. After the water is processed it flows back into the rivers downstream area downstream of the stilling basin. The problem with the approach flow will be discussed in the next section.

4.2 Approach flow to turbines

For this thesis the most interesting part of the construction is the region between the first weir field and turbine 2. Due to the height difference between the riverbed and the inlet to the turbines excessive turbulences and head losses will occur if the construction does not consider this problem. Another factor is the sediment bedplate between the riverbed and the elevated upstream floor upstream of the inlet which generates an additional height difference. The layout plan in Figure 38 shows the described region between turbine 2 and the weir.

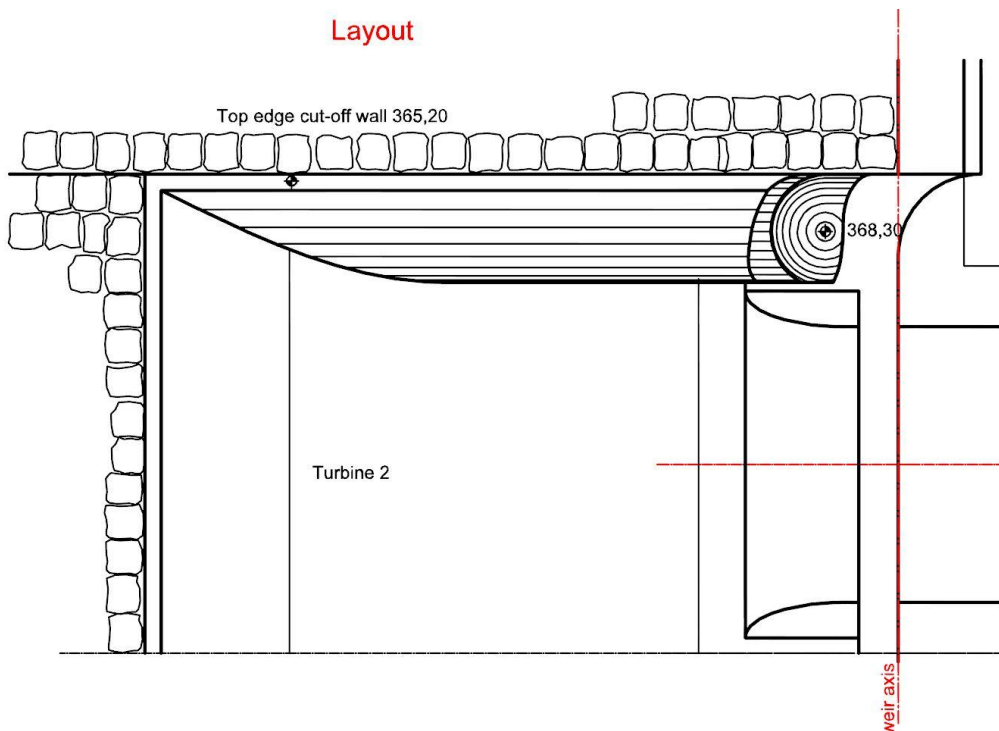


Figure 38: Layout turbine 2 [TU Graz, modified]

The longitudinal section in Figure 39 illustrates the same problem. The height difference between the top edge of the sediment bedplate and the bottom of the turbine inlet is 8.60 m. The bottom of the turbine inlet is at an elevation of 356.60 m.

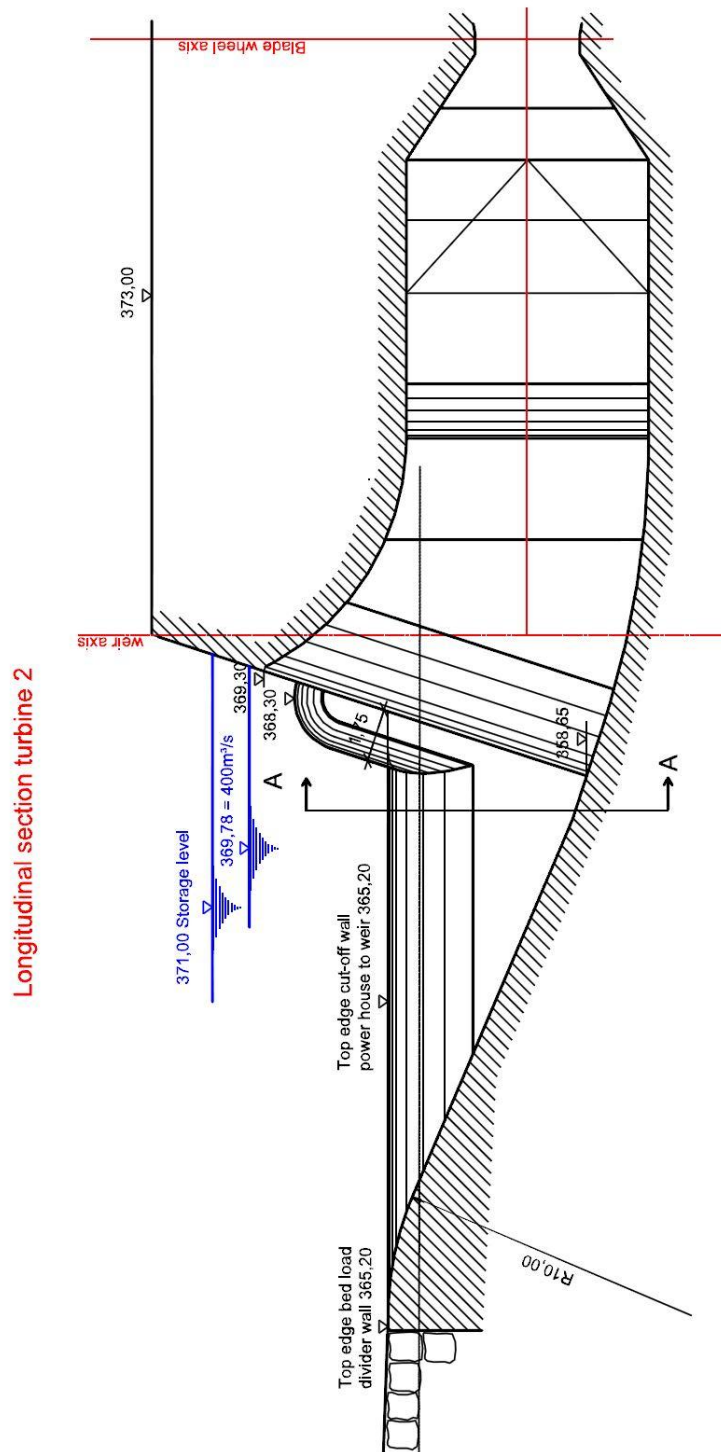


Figure 39: Longitudinal section turbine 2 [TU Graz, modified]

Another problem is the height difference between the top edge of the sediment bedplate and the riverbed. This distance is barely above one meter and it generates a flow in the upwards vertical direction and then after the bedplate the water flows downwards to the turbine inlets. Also the shape of this bedplate on both sides influences the water flow. On the left side, it is rectangular and on the right side it is a quarter circle with a radius of 2.80 m. Also the form of the separation pillar between the powerhouse and the first weir field matters. It is formed round three dimensional with a radius of 1.75 m and it is cut off vertically at the right side at 1.55 m. The pillar is also inclined 72 degrees to the horizontal (see Figures 39 and 40).

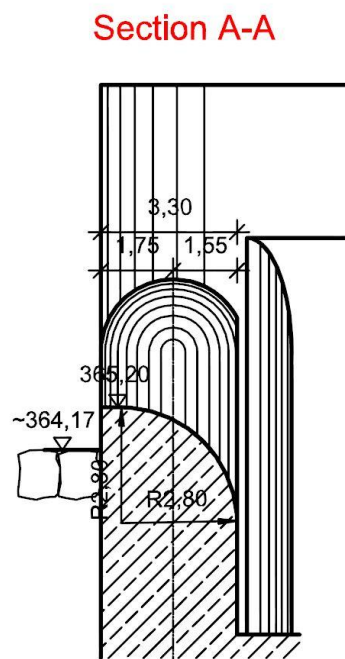


Figure 40: Section sediment control bedplate [TU Graz, modified]

The drawings in Figures 37 to 40 illustrate the current situation at the laboratory model Gratkorn. The sediment bedplate and the separation pillar have been modified to obtain satisfying results. Five improvements in this area have been done after numerical calculations and model testing in the laboratory. The measurements at the model Gratkorn are described in chapter 5 and they focus on these expected and calculated problems in the region near turbine 2.

5. ADV - Measurements at the model Gratkorn

The physical model Gratkorn (see Figure 41) was built in 2013. To build the 3D-model, cross sections in the downstream area, the headwater region and also in weir and turbine area were drawn by the laboratory staff. Some cross sections in the headwater area plus the weir axis cross section are adapted as the cross sections for the measurements. The distance between the individual sections is 62.5 cm which equates to 25 m in the nature. This distance is accurate enough to get the flow properties in the reservoir. Only between the weir axis and the first profile (PR 0.1-OW) two more cross sections are added to obtain more data in this specific area. The first cross section for the measurement is in the weir axis, shortly in front of the turbines (see Figure 42). It is chosen to measure the approach flow to the turbines. The next two cross sections (PR A-OW and PR B-OW) are new ones and they have a distance of 21 cm to each other. Then the next five profiles are adapted as cross sections for the measurement with a distance of 62.5 cm to each other.



Figure 41: Picture model Gratkorn

Figure 42 shows the layout plan of the headwater area of the model Gratkorn with the already existing cross sections and the two new cross sections PR A-OW and PR B-OW.

5.1 Turbines 1 and 2

5.1.1 Description of turbines 1 and 2

The measurements of both turbine inlets are carried out in the weir axis (see Figure 42). In this area the cross sections are quadratic with a side length of 21.0 cm which corresponds to 8.40 m in reality. A homogenous grid with a grid distance of 2.0 cm (0.80 m in prototype) is laid over this cross section. Near the boundaries the distance from the last measured point to the walls is just 1.5 cm to get as much information as possible about the flow conditions near the boundaries. In this area, measurements need to be checked for interferences or inaccuracies. The 100 measuring points are sufficient to provide a general picture of the velocity distribution.

In Figure 43 the cross section of turbine 1 and turbine 2 including the measuring grid is illustrated. The profile and the grid of turbine 1 and 2 are equal.

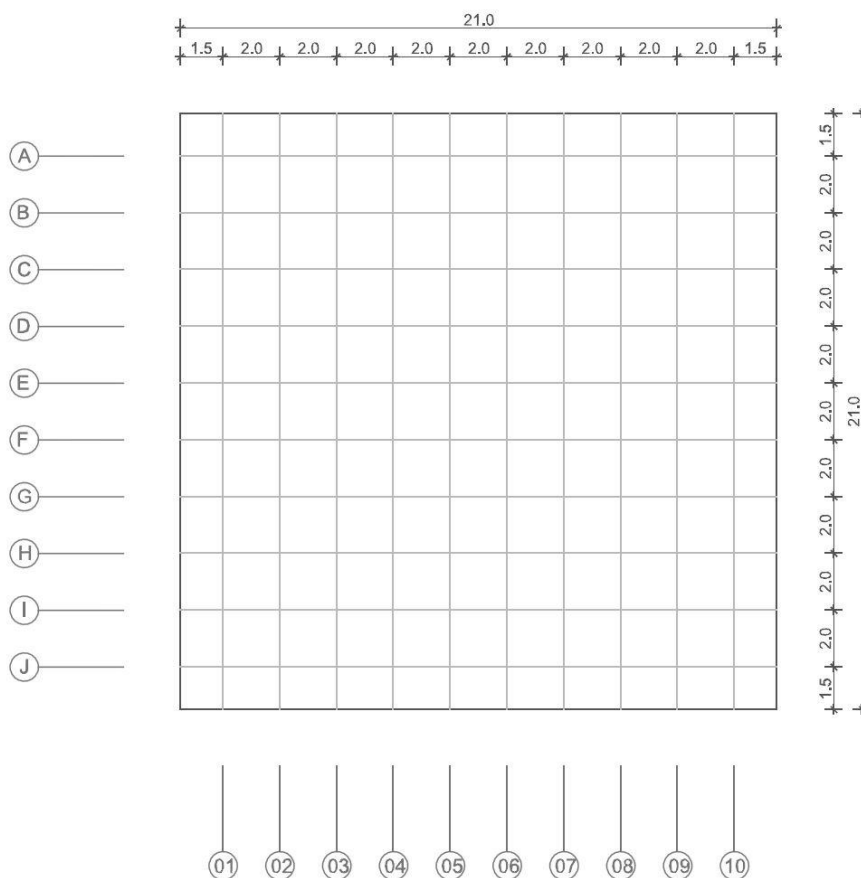


Figure 43: Cross section turbine 1 and 2 (dimensions in cm)

5.1.2 Results of turbine 1

Turbine 1 is on the right side of the powerhouse and the first one which is measured. Figure 44 illustrates the velocity distribution in x-direction (flow direction) at the inlet of turbine 1. The measurement starts 1.5 cm from the boundaries (see Figure 43) and the vectors demonstrate the direction and size of the velocities in y- and z-direction. The highest measured velocities occur at the top of the inlet and the lowest values are reached near the ground. Also the vectors point towards the centre and slightly to the left where turbine 2 is situated. The contour plot illustrates a regular incoming flow to turbine 1 with slightly higher velocities on the middle-right side and near the top.

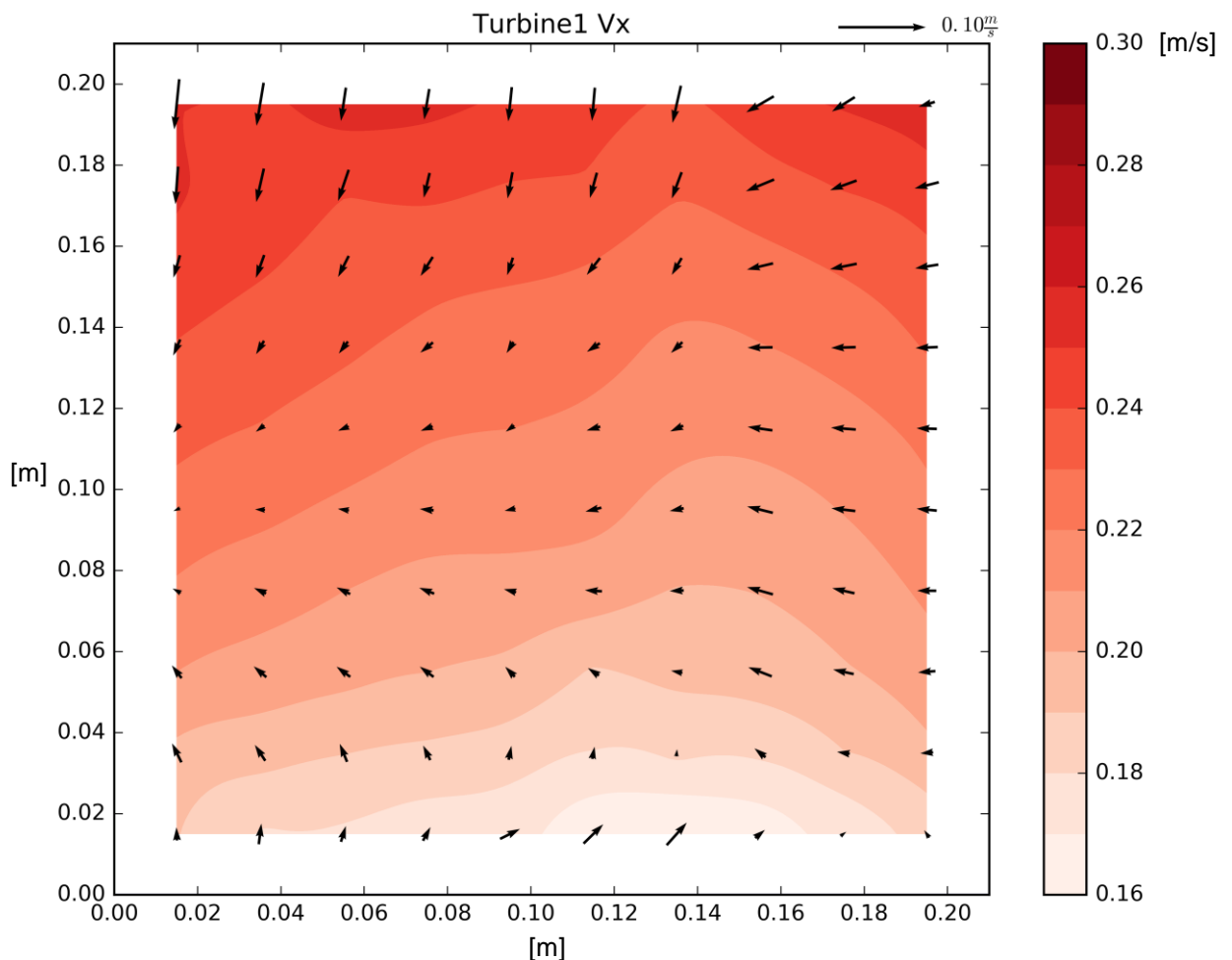


Figure 44: Velocities in x-direction at turbine 1

In Figure 45 the magnitude of the average velocities is shown. The contour plot is very similar to the x-velocity plot because velocities in x-direction are dominant in this case. Lowest velocities are also present at the bottom and the highest velocities are at the top, nevertheless the flow is fairly constant.

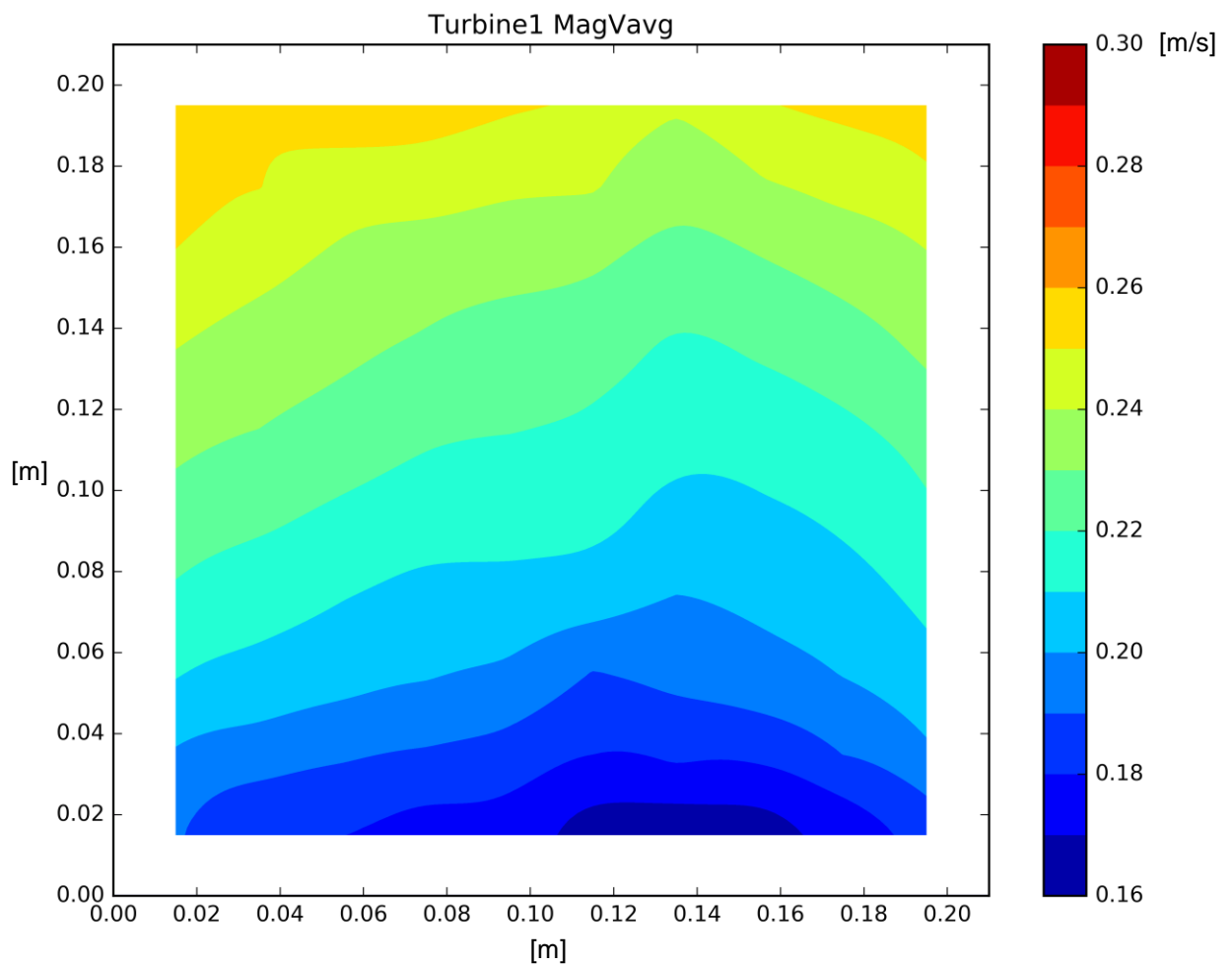


Figure 45: Magnitude of average velocities at turbine 1

In Table 3 the highest, lowest and in addition the average velocities are presented. As one can see the velocities in x-direction are the highest and most dominant ones, so the magnitude velocities also correspond to the x-values. The velocities in y- and z-direction are low in positive and negative direction. This also indicates a regular incoming flow to turbine 1.

Table 3: Max. and min. velocities turbine 1

	Max.	Min.	Average
X - direction	25.6 cm/s	16.1 cm/s	21.6 cm/s
Y - direction	2.3 cm/s	- 3.2 cm/s	- 1.3 cm/s
Z - direction	2.6 cm/s	- 5.7 cm/s	- 0.5 cm/s
Average V_{mag}	25.9 cm/s	16.7 cm/s	21.7 cm/s
Magnitude V_{avg}	25.8 cm/s	16.4 cm/s	21.8 cm/s

5.1.3 Results of turbine 2

To check the measurement time from the results in the laboratory flume another measuring time calculation like in chapter 3.2 is done for a few selective points. These special points are located in the top left corner near the walls where the highest change in velocity is expected. In this area measurement inaccuracies may occur. The result of point D4 is illustrated in Figure 46 as an example. The graph shows that a measuring time of 60 seconds is long enough to estimate average velocities. The rest of the selected points are attached at the end of the thesis in the appendix.

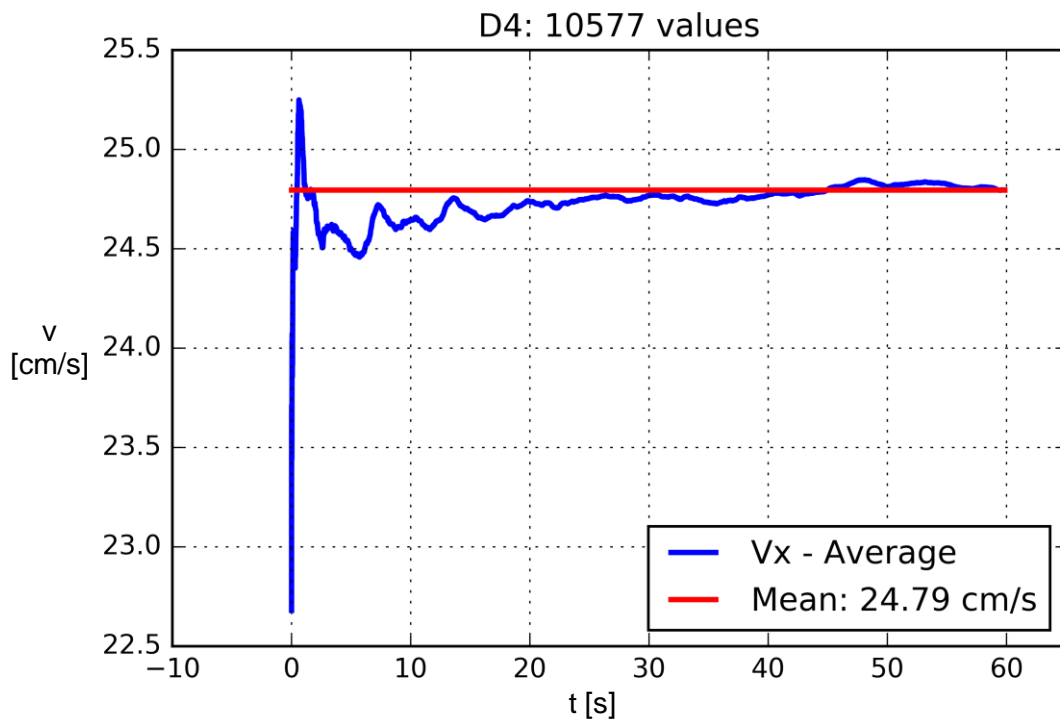


Figure 46: Point D4

At the inlet of turbine 2 turbulences are expected because of the sediment bedplate and the separation pillar. The results of the measurement (see Figure 47) confirm this assumption. Again the velocities at the bottom are lower than at the top but in this case the distribution is not constant. On the right side of the inlet the contour plot looks similar to the distribution in turbine 1 but the velocities are higher and the differences bigger. On the left side the influence of the bedplate and the pillar is visible. At the top left corner the velocities are very low; also they are higher at the middle and the bottom left side. After a short distance (a few centimetres) from the left wall the velocities get very high. The biggest difference in velocity is in the top left corner where in between a few centimetres the velocities rise from around 16 cm/s to nearly 26 cm/s. Also the vectors which describe the y- and z-velocities and their directions are very inconstant at the top left corner. They display high velocities in different directions, also an evidence of turbulences.

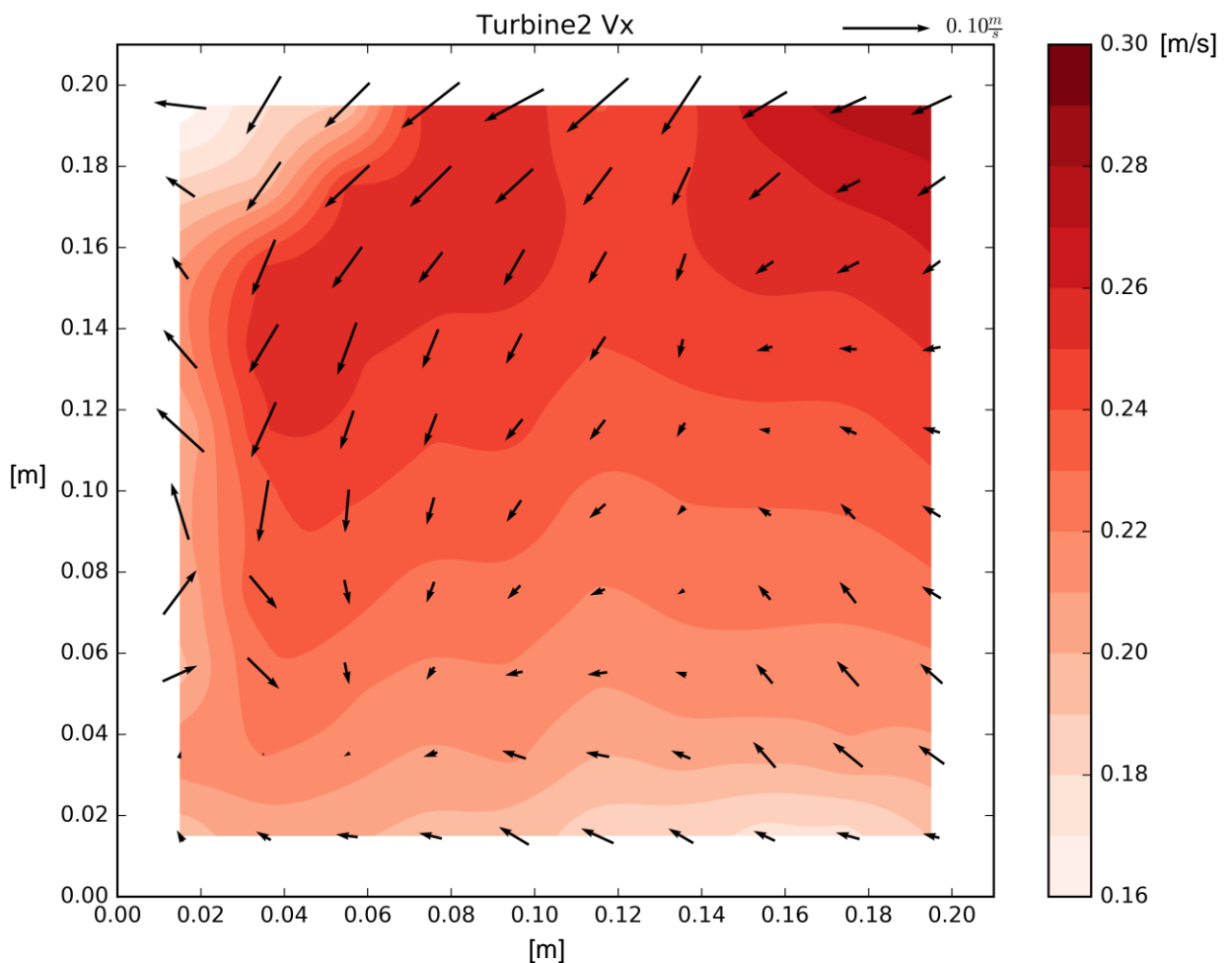


Figure 47: Velocities in x-direction at turbine 2

The magnitude plot of the average velocities (see Figure 48) at the inlet of turbine 2 illustrates the same result. High velocities measured at the top except at the top left corner where the velocities are very low. In this top left corner the magnitude of the average velocities also rises from around 16 cm/s to 26 cm/s within a short distance. Also at the left wall the velocities are much lower than on the right side. Again this indicates effect of the sediment bedplate and the pillar. The water has to flow over the barrier and then down the left wall, so a uniform incoming flow to turbine 2 is unfeasible.

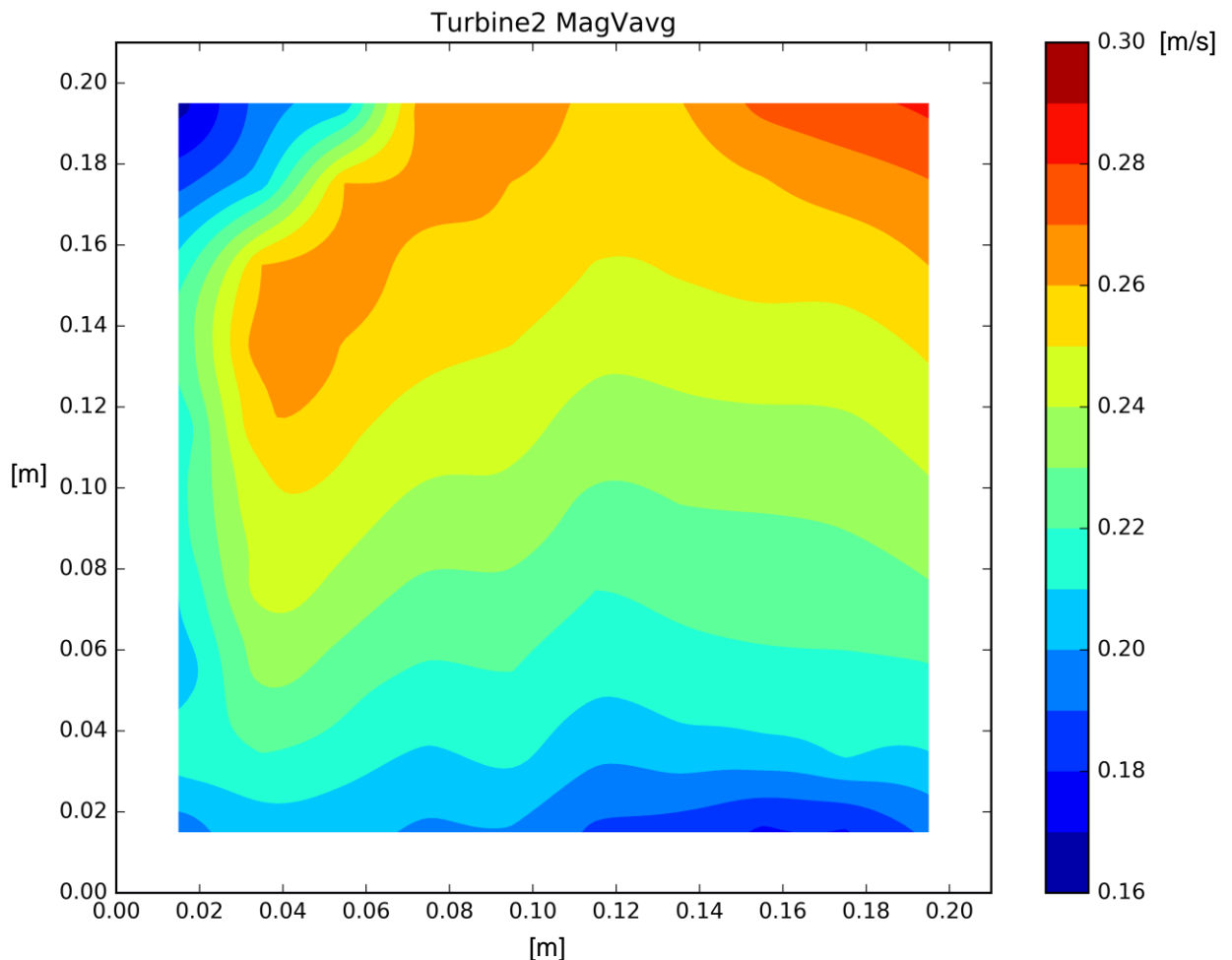


Figure 48: Magnitude of average velocities at turbine 2

In Table 4 the maximum, minimum and average velocities for all directions and also the magnitudes are displayed. The maximum velocities in each direction are higher than at turbine 1 and the minimum velocities are lower. This results in higher velocity differences. Also the average velocities are higher than at turbine 1. However the velocities in x-direction are dominant again but the y- and z-velocities have much more influence on the outcome. As a result a perfectly uniform flow to turbine 2 is not achieved.

Table 4: Max. and min. velocities turbine 2

	Max.	Min.	Average
X - direction	27.8 cm/s	15.5 cm/s	22.7 cm/s
Y - direction	4.0 cm/s	- 7.1 cm/s	- 2.2 cm/s
Z - direction	6.5 cm/s	- 7.1 cm/s	- 1.2 cm/s
Average V_{mag}	28.7 cm/s	18.1 cm/s	23.2 cm/s
Magnitude V_{avg}	28.2 cm/s	16.6 cm/s	23.5 cm/s

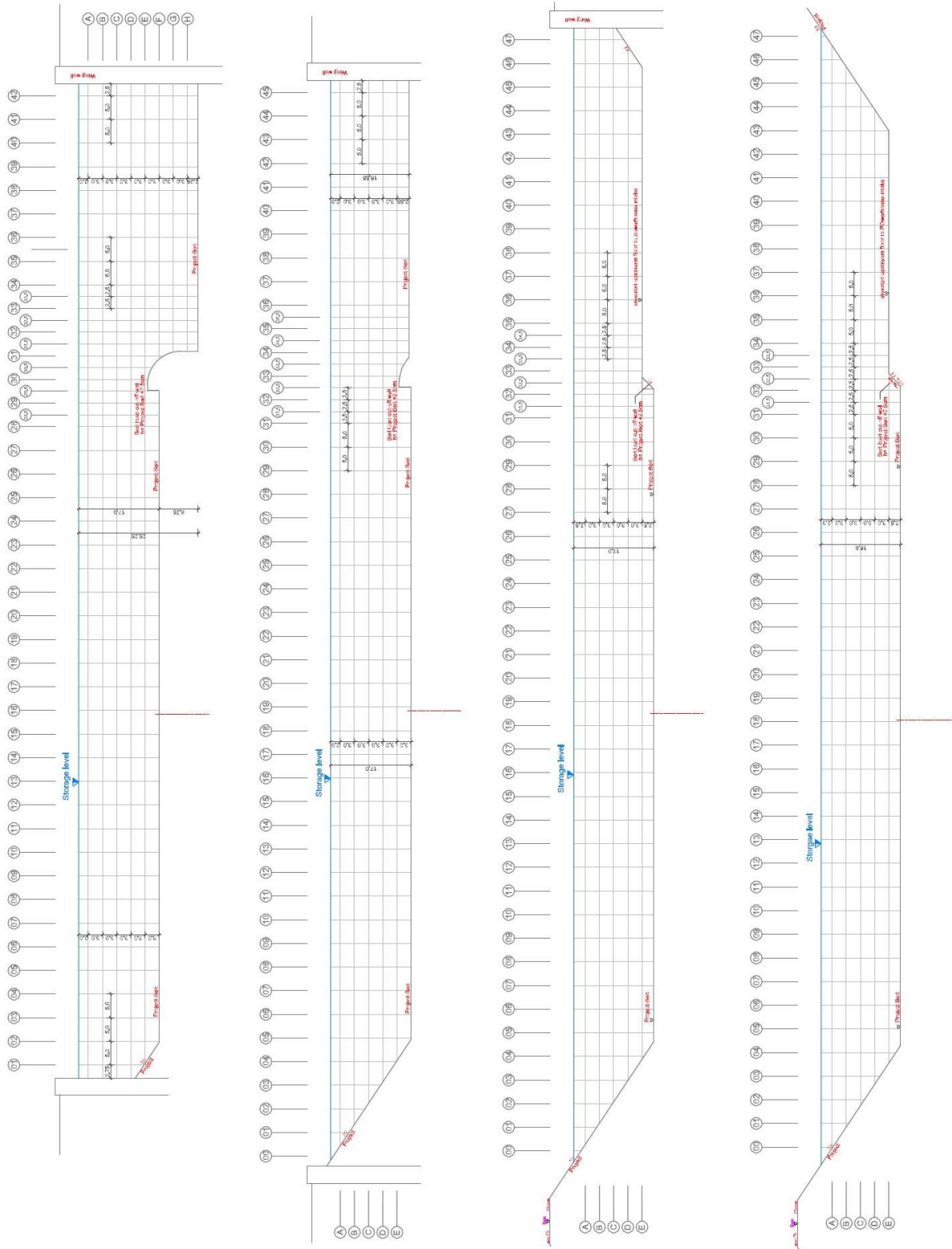
5.2 Profile PR A - OW

5.2.1 Description of profile PR A - OW

The first cross section across the whole upstream area is situated 21 cm upstream from the weir axis (see Figure 42). A raster of 5 cm times 3 cm is chosen to have enough points to create accurate velocity contour plots (see Figure 49). Furthermore, the difficulties near the bottom, surface and walls are eliminated with these distances. Also there should not be too many points because then the measurement will take too long (60 seconds for each point). With this grid there are 5 horizontal rows of points from the bottom to the water surface and 42 vertical lines from the left bank to the right bank. Furthermore, in the area of the sediment bedplate and the separation pillar the grid is refined for better identification of the turbulence flows. In this area the grid is 3 cm times 2.5 cm, basically the vertical lines are doubled. Six additional vertical lines are added to cover this particular region. With this grid all velocities in cross section PR A-OW are covered, especially on the right side of the profile. On the left side of profile A very low velocities near the weir fields are expected and so the grid is coarsened. In this area it is adequate to measure just every second or third vertical line of points. So all in all there are more than 200 points to measure and post-process. The cross section plan in Figure 49 illustrates the grid of points which is applied.

It should be added that this procedure is done for all the other cross sections in the same way. The underlying grid is a raster of 3 cm times 5 cm which is modified in the area of the sediment bedplate and separation pillar. In this particular region the number of vertical lines is doubled to generate a tighter grid. It should be stressed that the further away from the weir axis the cross section is, the less vertical lines are added. So for cross section B five additional vertical lines are added, for section 0.1 there are four additional lines and for section 1.0 there are three more vertical lines (see Figures 50 to 52). For the remaining cross sections no additional lines are applied, the grid of 3 cm time 5 cm stays the same across the whole section. Just on the left sides of the sections the numbers of measured vertical lines decrease according to measuring results of

the velocities. The drawings of each cross section in a certain scale are presented in the appendix.

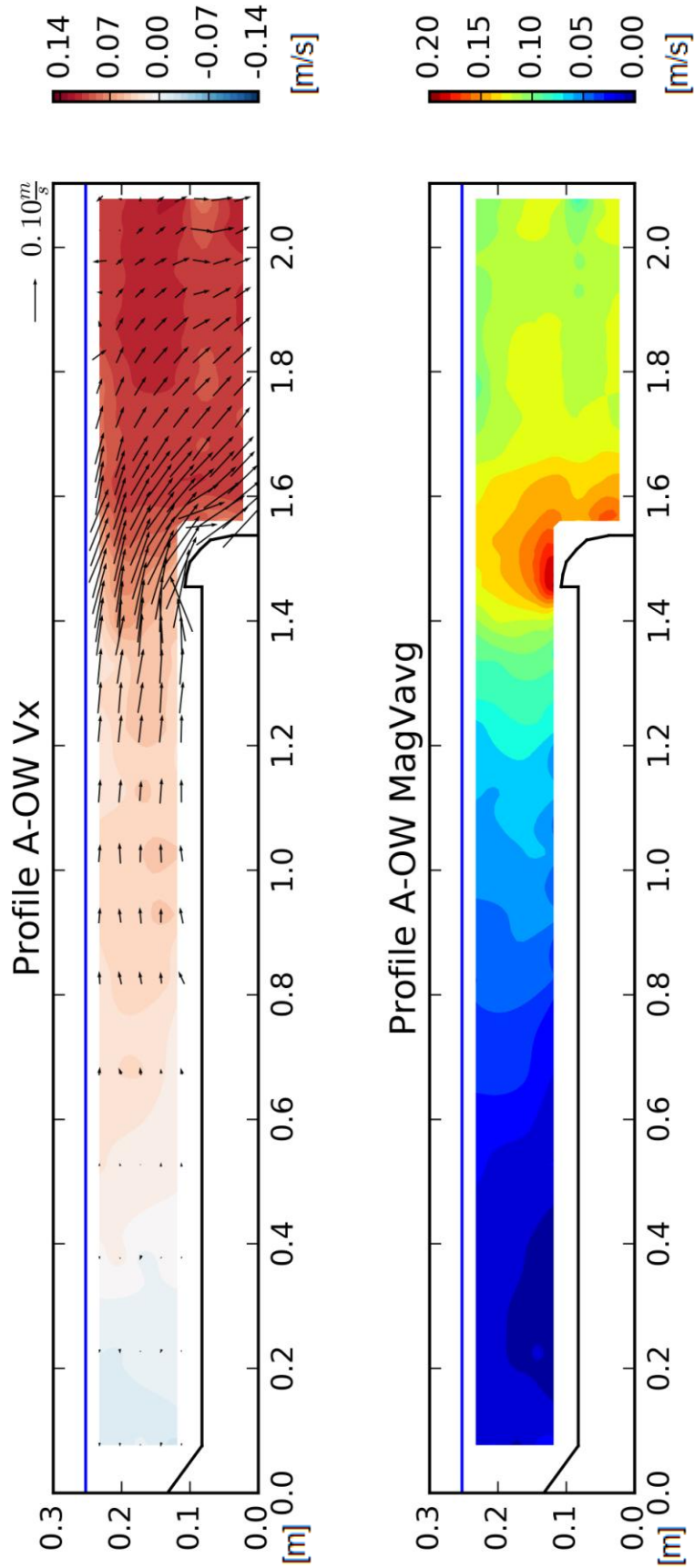


Figures 49, 50, 51 and 52: Cross sections PR A-OW, PR B-OW, PR 0.1-O and, PR 1.0-OW

5.2.2 Results of profile PR A - OW

The velocity contour plots of profile A - OW describe a very turbulent flow in the area of the sediment bedplate and the separation pillar. In this region the highest velocities in each direction occur, even though there are just negative y- and z-velocities, due to the coordinate system of the Vectrino probe. The highest x-velocities appear at the right side of the cross section which leads to the intakes of the turbines. Near the vertical separation wall, due to the inclination to the turbines, the x-velocities decrease rapidly but the velocities in z- and y-direction are increase in this area. The highest y-velocities occur directly above the sediment bedplate because the water has to flow over this underwater barrier to get to the turbine intakes. Further away from the left wall of the intakes the y-velocities decrease again. The highest z-velocities appear near the left wall of the intakes where the flow points downwards. On the right side of the intakes the z-velocities stay even with no major divergences. Also the vectors in the contour plot point out these processes. Most of the vectors point to the right side and also downwards which explains the negative y- and z-velocities. Furthermore, it has to be pointed out that at the left side of the cross section very low velocities in every direction can be observed. On the very left side, very small velocities to the left and backwards against the main stream occur, the flow changes its direction after "hitting" the weirs. The closer the measurement gets to the sediment bedplate, seen from the left side, the higher the velocities to the turbine intakes get.

Figures 53 and 54 show these water flows. Figure 53 shows the x-velocities with vectors describing the velocities in the other two directions. Figure 54 demonstrates the magnitude of the average velocities appearing in the channel.



Figures 53 and 54: Velocities in x-direction and magnitude of V-average at profile PR A - OW

In Figure 54 the overall velocity distribution is displayed. At the left side of the cross section nearly no water flow appears. Near the sediment bedplate the magnitude of the velocities reach a maximum and on the right side of the turbine intakes they finally get uniform again.

The same results are shown in Table 5 which plots the maximum, minimum and average velocity in each direction and in addition the magnitude velocities. In x-direction the highest velocities are present in the area of the turbine intakes while the lowest ones appear on the very left side of the cross section near the bottom. The highest y-velocities occur near the bottom right before the sediment bedplate. Near the left bank and the right bank they are very low. Z-velocities are very high near the left wall of the intakes and in all other areas they are also quite low. In some areas at profile PR A-OW the velocities in y-direction are higher than in x-direction. That means that the highest velocity is no longer perpendicular to the emitting direction of the ADV device. Nevertheless the measurements are accurate and the data valid.

Table 5: Max. and min. velocities profile PR A - OW

	Max.	Min.	Average
X - direction	12.2 cm/s	- 2.4 cm/s	7.2 cm/s
Y - direction	1.4 cm/s	- 18.2 cm/s	- 5.4 cm/s
Z - direction	5.1 cm/s	- 11.9 cm/s	- 2.5 cm/s
Average V_{mag}	19.6 cm/s	1.0 cm/s	10.6 cm/s
Magnitude V_{avg}	19.3 cm/s	0.4 cm/s	10.4 cm/s

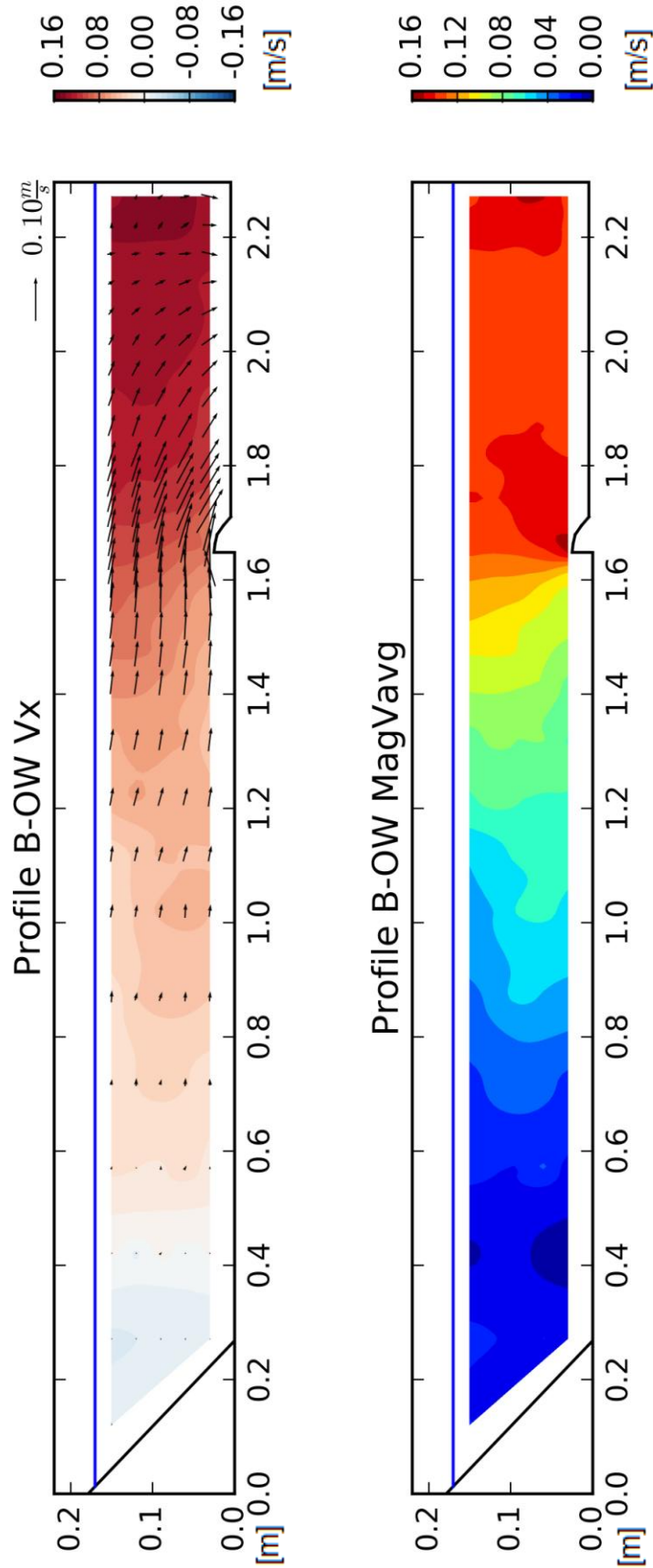
5.3 Profile PR B – OW

5.3.1 Description of profile PR B - OW

Cross section PR B-OW is located between profiles PR A-OW and PR 0.1-OW and it is 42 cm upstream from the weir axis. This profile is near the start of the inclination of the inlet to the turbines. The measuring grid is the same as described before and is shown in Figure 50 (see page 59). On the right side of the turbine inlet there is a wing wall and the left side of the cross section is limited with an inclined river bank.

5.3.2 Results of profile PR B – OW

The main flow in this profile is the flow in x-direction (see Figure 55); therefore the x-velocities are the dominant ones. On the very right side of the cross section the highest x-velocities occur and on the left side there is nearly no water movement. To the right of the sediment bedplate the x-velocities are constantly distributed and on the left side of the bedplate they decrease rapidly. The velocities in y-direction are very low everywhere in the profile except the area around the sediment bedplate because in this region the water has to flow over this barrier to the inlet of the turbines. Also on the very right side of the turbine inlets there is nearly no movement in y-direction. The velocities in z-direction are also very low on the left side of the profile but in front of the bedplate they rise in the positive direction (towards water surface) and after the bedplate they are high in negative direction (towards bottom). That also indicates the water flow over the sediment bedplate. In the area of the turbine intakes the z-velocities are uniformly distributed, they rise towards the ground because of the inclination to the intakes. This all can be seen in Figure 55 where the contour plot of x-velocities is present, the y- and z-velocities are indicated with vectors. In Figure 56 the distribution of the magnitude of the average velocities is present and it illustrates the same result: very low velocities on the left side and uniformly distributed velocities on the right side of the bedplate. Near the region of the sediment bedplate the velocities rise moderately and close in front of it they raise rapidly because of higher y- and z-velocities.



Figures 55 and 56: Velocities in x-direction and magnitude of V-average at profile PR B - OW

Table 6 compares the highest and lowest velocities in every direction of this profile. The highest velocities occur in x-direction and slightly lower are the maximums in y-direction. Velocities in z-direction are small compared to the other two directions.

Table 6: Max. and min. velocities profile PR B - OW

	Max.	Min.	Average
X - direction	15.0 cm/s	-2.2 cm/s	8.7 cm/s
Y - direction	1.0 cm/s	-12.5 cm/s	-4.5 cm/s
Z - direction	2.5 cm/s	-6.1 cm/s	-1.4 cm/s
Average V_{mag}	15.2 cm/s	1.1 cm/s	10.7 cm/s
Magnitude V_{avg}	15.4 cm/s	0.1 cm/s	10.5cm/s

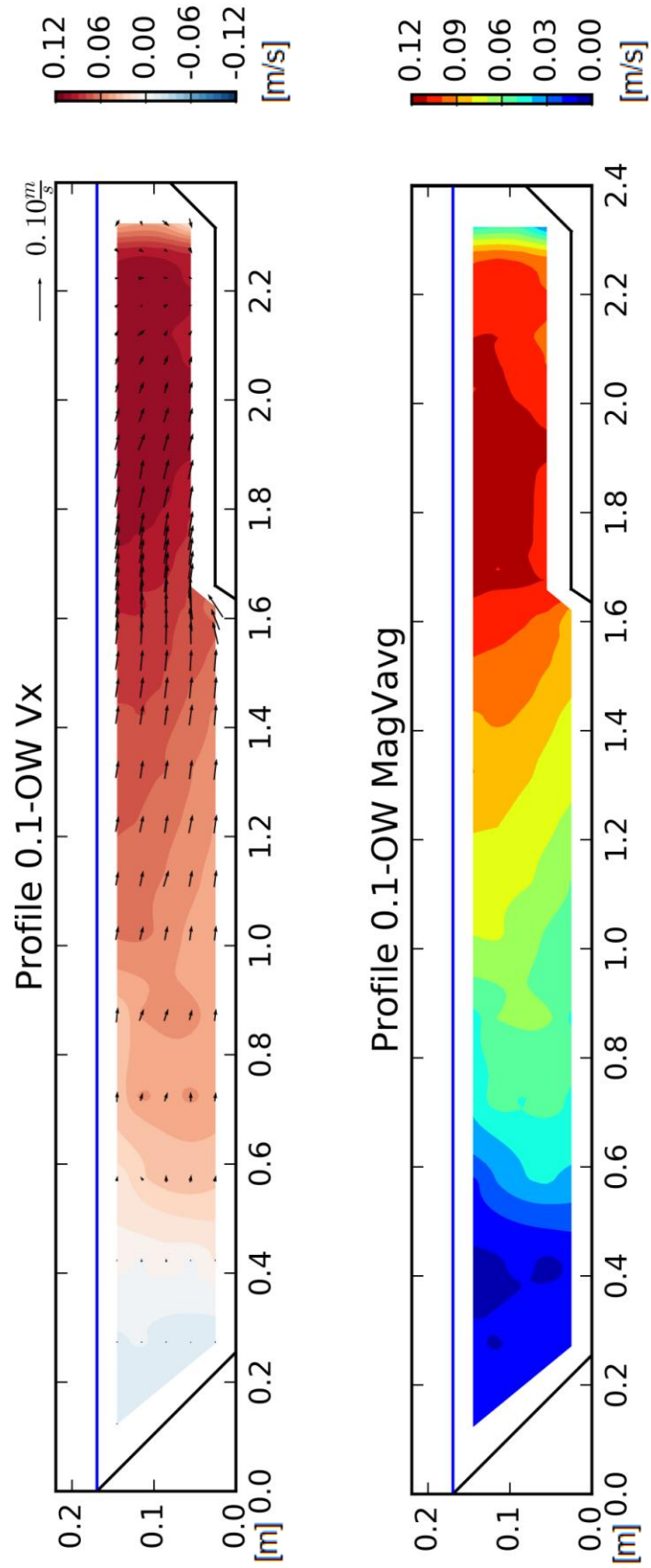
5.4 Profile PR 0.1 - OW

5.4.1 Description of profile PR 0.1 - OW

The cross section PR 0.1-OW is the first profile which was used to build the model in the laboratory. It is located 62.5 cm upstream from the weir axis and is one of the widest cross sections. All in all there are 47 vertical lines of measuring points as shown in Figure 51 (see page 59). On the right side of the profile there is a vertical wing wall and on the left side the river is limited by an inclined river bank. It is the first cross section without a height difference after the sediment bedplate on the right side. The right side of the ground (area of turbine inlet) is situated 2.5 cm higher than the rest of the riverbed. This sediment bedplate is formed with a vertical wall in this profile and it changes to an inclination of 45 degrees moving upstream from the weir axis.

5.4.2 Results of profile PR 0.1 – OW

In this cross section the main flow is located on the right side on the elevated floor towards the intakes. Velocities in x-direction are dominant but y-velocities are also very high near the sediment bedplate. The x-velocities are very high on the right side of the profile and get lower in the centre and very low and even negative on the left side. On the very right side the x-velocities get very low too because of the form of the wing wall on the right side; the water flow is held back. Velocities in y-direction are very high in the area around the sediment bedplate and get lower to the left and right bank. They face towards the turbine intakes. Velocities in z-direction are very low across the whole profile except in front of the sediment bedplate. In this area the water has to flow over this barrier, therefore velocities in y- and z-direction increase significantly. In the rest of the cross section z-velocities are distributed uniformly and they are slightly higher near the turbine intakes than in the rest of the profile. These results are evident in Figures 57 and 58. The velocities in x-direction are shown with vectors for the y- and z-velocities and also the magnitude of the average velocities is evident. The magnitude contour plot displays also main flow on the right side and lower velocities towards the left side.



Figures 57 and 58: Velocities in x-direction and magnitude of V-average at profile PR 0.1 - OW

In Table 7 the maximum, minimum and average values for each flow direction are illustrated and they deliver the same results. Flow in x-direction is dominant and there are also high velocities in y-direction. In z-direction there are low velocities; with some peaks occurring in the area of the sediment bedplate.

Table 7: Max. and min. velocities profile PR 0.1 - OW

	Max.	Min.	Average
X - direction	11.0 cm/s	-1.9 cm/s	7.3 cm/s
Y - direction	2.3 cm/s	-7.2 cm/s	-3.4 cm/s
Z - direction	3.5 cm/s	-1.8 cm/s	-0.5 cm/s
Average V_{mag}	11.9 cm/s	1.2 cm/s	8.7 cm/s
Magnitude V_{avg}	11.8 cm/s	0.6 cm/s	8.5 cm/s

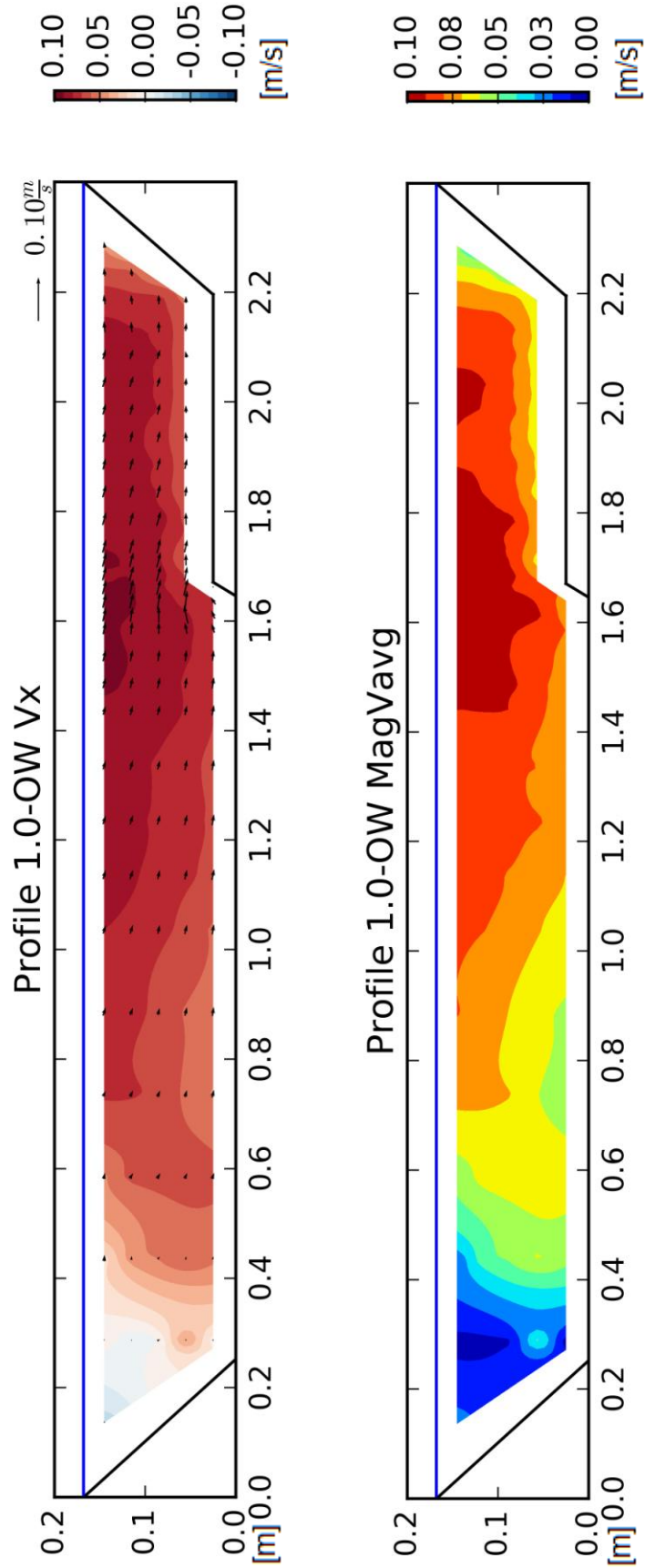
5.5 Profile PR 1.0 - OW

5.5.1 Description of profile PR 1.0 - OW

The cross section of profile PR 1.0-OW is located 125 cm upstream from the weir axis and its grid is evident in Figure 52 (see page 59). It is the last profile where the measuring grid is tighter in the area of the sediment bedplate. This cross section is limited with inclined river banks on both sides and the upstream floor to the turbine intakes on the right side is elevated by 2.5 cm. Over the whole cross section there are 46 vertical measuring lines and five horizontal ones.

5.5.2 Results of profile PR 1.0 - OW

Further upstream from the weir axis the influence of the sediment bedplate on the flow conditions drops. In this profile the x-velocities are dominant and the other two flow directions are quite small compared to the main flow. Also the highest x-velocities move more to the centre of the profile. On the very left side there are very small and even negative x-velocities in the top left corner. Velocities in y-direction are small across the whole profile and they are uniformly distributed slightly rising near the sediment bedplate. They get lower towards the left side of the cross section but there is no significant velocity difference. Velocities in z-direction are even lower and also distributed uniformly. There is just one peak of higher z-velocities right in front of the sediment bedplate where the water has to flow up over the barrier. These results are present in Figure 59 which shows the contour plot of x-velocities with vectors for y- and z-velocities. In Figure 60 a contour plot of the magnitude of the average velocities is present and it delivers the same result: the main flow is orientated near the centre of the profile and low velocities only occur on the very left side. Also the influence of the y- and z-velocities near the sediment bedplate is not recognisable.



Figures 59 and 60: Velocities in x-direction and magnitude of V-average at profile PR 1.0 - OW

The peak and average velocities in Table 8 illustrate the same outcome. Main flow direction is the x-direction and the other two velocities are quite small compared to the x-velocities. Also the magnitude velocities and the x-velocities become increasingly indistinguishable.

Table 8: Max. and min. velocities profile PR 1.0 - OW

	Max.	Min.	Average
X - direction	9.3 cm/s	-2.5 cm/s	7.1 cm/s
Y - direction	0.4 cm/s	-4.7 cm/s	-2.3 cm/s
Z - direction	1.1 cm/s	-1.1 cm/s	-0.4 cm/s
Average V_{mag}	10.0 cm/s	1.8 cm/s	7.8 cm/s
Magnitude V_{avg}	9.8 cm/s	0.4 cm/s	7.6 cm/s

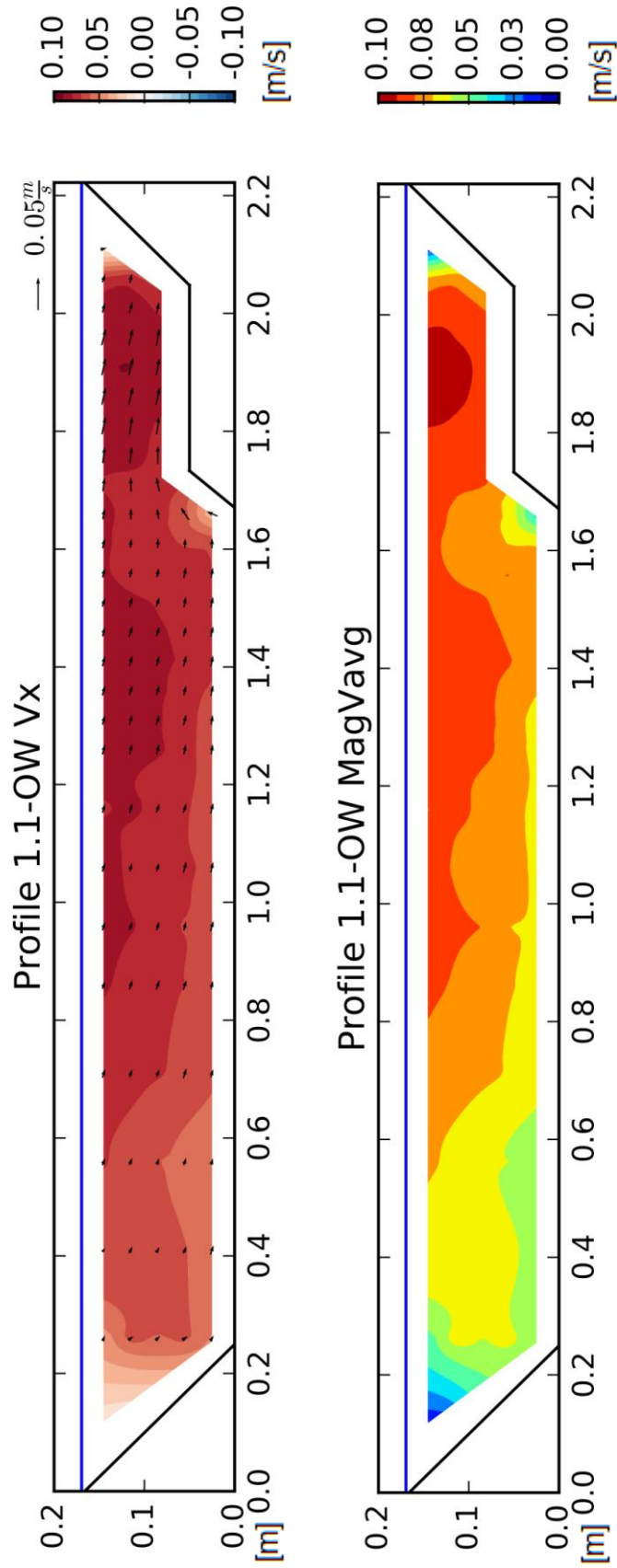
5.6 Profile PR 1.1 - OW

5.6.1 Description of profile PR 1.1 - OW

This profile is located 187.5 cm upstream from the weir axis and the measuring grid is five times three centimetres across the whole cross section. On both sides of the river there are dams, so the river banks are inclined. The upstream river bed is elevated by 2.5 cm on the right side of the profile. All in all there are 43 vertical measuring lines and five horizontal ones. The drawing of this cross section is evident in the appendix.

5.6.2 Results of profile PR 1.1 - OW

In this profile the x-direction is the main flow direction and the other two flow directions are negligibly small compared to the main one. The x-velocities are at highest in the centre of the cross section and above the elevated floor to the turbine intakes. There is a nearly uniform distribution of x-velocities, solely in the top left and top right corner lower velocities occur. Velocities in y-direction are very low across the whole cross section although above the elevated floor towards the turbine intakes they are slightly higher than in the rest of the profile. In z-direction the velocities are the lowest, there is just a small peak right in front of the sediment bedplate where the water flow has to go upwards. The Figures 61 and 62 describe these flow conditions. The x-velocity contour plot displays the main flow direction and the vectors point towards the related y- and z-directions. The magnitude plot of the average velocities demonstrates the main flow near the centre of the profile and there is also an intense flow on the right side towards the turbine intakes. Just on the very left and right side there is little to no water movement.



Figures 61 and 62: Velocities in x-direction and magnitude of V-average at profile PR 1.1 - OW

The numbers in Table 9 lead to the same conclusion. Velocities in y- and z-direction are low and the x-velocities are the dominant ones. The influence of the y- and z-velocities is nearly negligible.

Table 9: Max. and min. velocities profile PR 1.1 - OW

	Max.	Min.	Average
X - direction	9.1 cm/s	0.5 cm/s	7.3 cm/s
Y - direction	0.1 cm/s	-2.8 cm/s	-1.6 cm/s
Z - direction	1.7 cm/s	-1.7 cm/s	-0.4 cm/s
Average V_{mag}	9.6 cm/s	2.1 cm/s	7.6 cm/s
Magnitude V_{avg}	9.5 cm/s	0.6 cm/s	7.5 cm/s

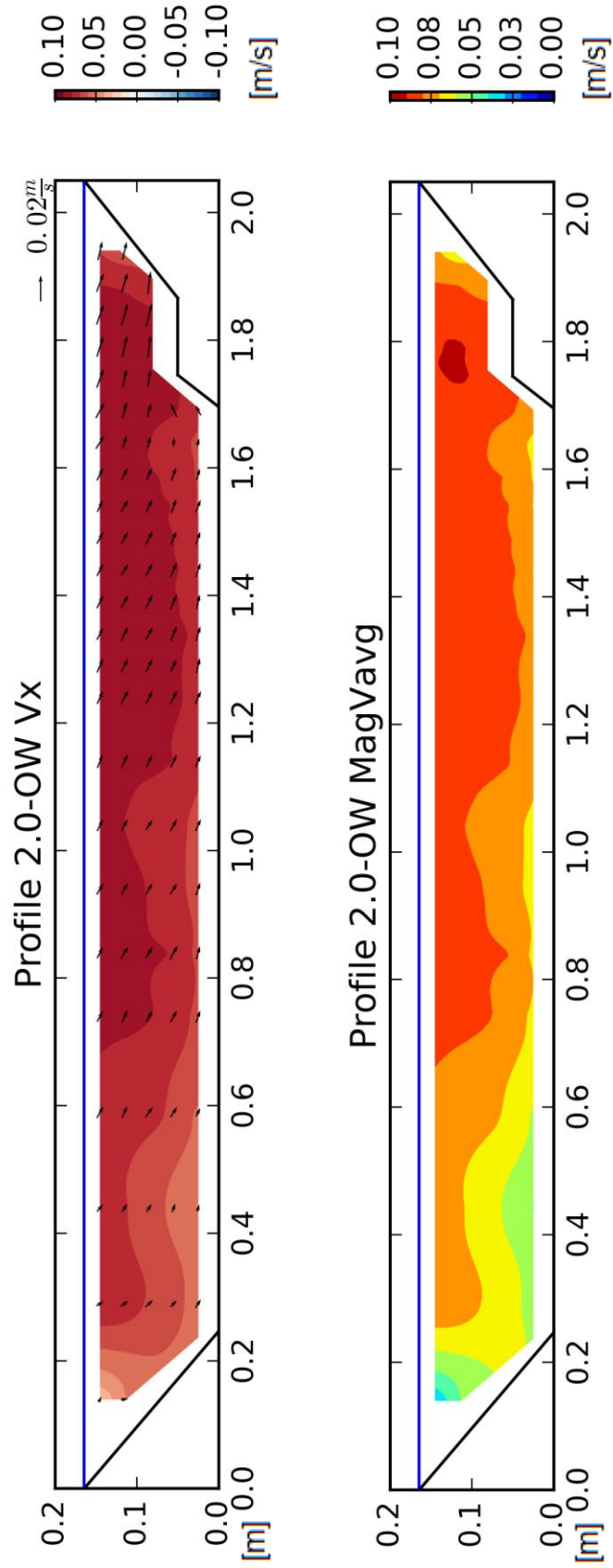
5.7 Profile PR 2.0 - OW

5.7.1 Description of profile PR 2.0 - OW

Cross section PR 2.0-OW is the last profile with an elevated upstream river bed on the right side towards the turbine intakes. It is located 250 cm upstream from the weir axis and it has 39 vertical measuring lines and five horizontal ones with a grid of five times three centimetres. This profile is limited with inclined river banks (dams) on both sides. The drawing is evident in the appendix.

5.7.2 Results of profile PR 2.0 - OW

Profile 2.0-OW shows a nearly uniform velocity distribution across the whole cross section. The influence of the sediment bedplate is just marginal and the main flow is located near the centre of the profile. Velocities in x-direction are very dominant and also evenly distributed. Just on the very left side the x-velocities are lower than in the rest of the cross section. Velocities in y-direction are very low across the whole profile. The highest y-velocities occur on the right side of the profile above the elevated floor towards the turbine intakes. Velocities in z-direction are insignificant; they are around zero across the whole profile. Most of the time they are slightly negative but in the area of the sediment bedplate an infinitesimally small flow upwards is recognisable. The two contour plots in Figures 63 and 64 demonstrate these results. In the magnitude plot (see Figure 64) the flow distribution is displayed. The main flow area ranges from the centre of the profile to the area near the sediment bedplate. It nearly looks like the flow distribution in a trapezoidal cross section but it is shifted slightly to the right of the centre.



Figures 63 and 64: Velocities in x-direction and magnitude of V-average at profile PR 2.0 - OW

The maximum and minimum values in Table 10 also explain these outcomes. Main flows are in x-direction and the velocities in y- and z-direction oscillate around zero on a very low scale. The peak and average magnitude velocities are also very close to the x-velocities.

Table 10: Max. and min. velocities profile PR 2.0 - OW

	Max.	Min.	Average
X - direction	9.0 cm/s	3.0 cm/s	7.8 cm/s
Y - direction	-0.1 cm/s	-1.8 cm/s	-1.0 cm/s
Z - direction	0.5 cm/s	-0.7 cm/s	-0.4 cm/s
Average V_{mag}	9.2 cm/s	3.4 cm/s	7.9 cm/s
Magnitude V_{avg}	9.1 cm/s	3.1 cm/s	7.8 cm/s

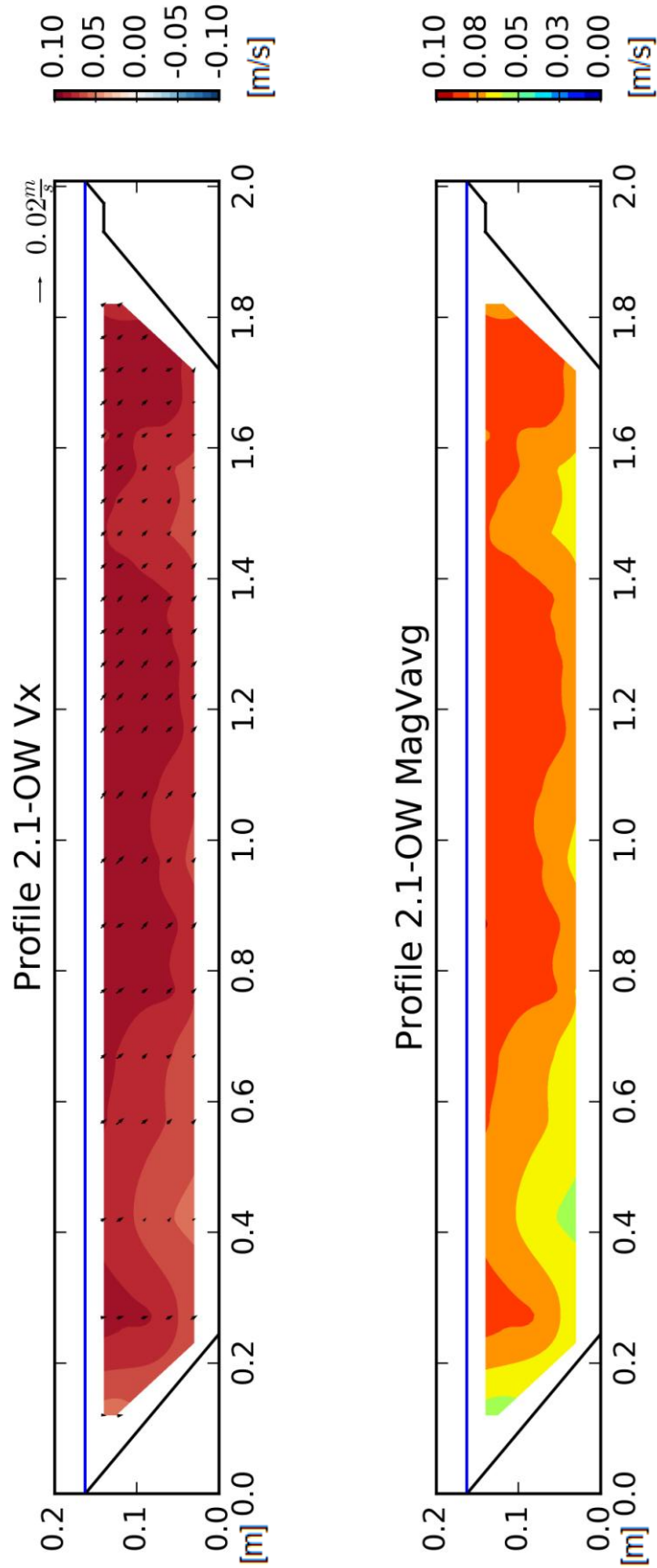
5.8 Profile PR 2.1 - OW

5.8.1 Description of profile PR 2.1 - OW

This cross section is located 312.5 cm upstream from the weir axis and is limited with dams on both sides. On the right side near the water surface there is a bench which is part of the fish pass. This profile is trapezoidal and has a measuring grid of five times three centimetres with 37 vertical lines and four horizontal ones. The drawing is evident in the appendix.

5.8.2 Results of profile PR 2.1 - OW

The measurements of this cross section deliver a very similar result to the flow conditions expected in a straight trapezoidal river profile. The highest velocities in flow direction are near the centre of the river and towards the ground the velocities decrease. The flow distribution is uniform; there is just a very small influence of the turbine intakes noticeable on the right side. Velocities in y- and z-direction are very low oscillating around zero. They point downwards to the right because of the inclination of the river bed and the little influence of the turbine intakes. Velocities in flow direction (x-velocities) are absolutely dominant and the influence of y- and z-velocities is infinitesimally small. This result can also be seen in Figures 65 and 66. The vectors in the x-velocity contour plot indicate the y- and z-velocities and they are negligible small compared to main flow velocities. Also in the magnitude plot of all velocities the influence of these two velocities is not recognisable. The distribution of the magnitude contour plot is identical to the distribution of the x-velocity contour plot.



Figures 65 and 66: Velocities in x-direction and magnitude of V-average at profile PR 2.1 - OW

The results of profile PR 2.1-OW are also summarized in Table 11. Velocities in y- and z-direction are quite small, nearly zero. The velocities in x-direction are the dominant ones and therefore the magnitude velocities correlate to the x-velocities. There is no noticeable influence of the other two velocity directions on the magnitude velocity plot.

Table 11: Max. and min. velocities profile PR 2.1 - OW

	Max.	Min.	Average
X - direction	9.1 cm/s	5.2 cm/s	7.8 cm/s
Y - direction	0.1 cm/s	-0.6 cm/s	-0.4 cm/s
Z - direction	-0.2 cm/s	-0.6 cm/s	-0.5 cm/s
Average V_{mag}	9.2 cm/s	5.4 cm/s	8.0 cm/s
Magnitude V_{avg}	9.1 cm/s	5.2 cm/s	7.9 cm/s

5.9 Horizontal contour of velocity

The upstream flow distribution is generated with the points from the centre row of all seven upstream cross sections. This means the result illustrates the flow conditions 8.5 cm (3.40 m in prototype) above the river bed and 8.5 cm below the water surface. The area covered by the contour plots ranges from the bend between the bank and the river bed on the left side to the bend of the bank and the elevated river bed in front of the turbine intakes on the right side.

The horizontal contour plots of velocity are shown in Figures 67 and 68. It has to be pointed out that over the whole layout the x-velocities are dominant, just in a few small area peaks in y- and z-direction occur. On the orographic left side of the storage area all velocities are much lower than on the right side, especially directly upstream of the weirs. In this region the velocities are near zero and they reach a maximum on the right side of the storage area in front of the turbine intakes. The highest velocities in y-direction occur directly above of the separation wall, in z-direction the maximums are also reached in this region. The influence of this cut-off wall for y-velocities is recognized as far as the fifth profile (PR 1.1-OW). Everywhere else the y-velocities are uniformly distributed. The influence of the cut-off wall for the z-velocities is even smaller. After the third profile (PR 0.1-OW) no influence is recognized anymore. Apart from that the inclination to the turbines is of high influence to the velocities in z-direction. The velocities in x-direction also rise towards the turbine intakes and reach their maximum in this area. A stream towards the turbine intakes can be identified and on the left side of the storage area the velocities drop. There is even a backflow in front of the last weir field on the left side. The separation wall does not have a significant influence on the x-velocities but there is some kind of vortex to the turbine intakes. The magnitude plot in Figure 66 shows the same results. There is nearly no flow on the left side in front of the weirs and maximum velocities directly in front of the turbine intakes. Also a nearly uniform distribution of water flow is evident in the last measured profile (PR 2.1-OW). The influences of the separation wall and the inclination to the turbine intakes are also apparent. Even the maelstrom to the turbines is clearly evident in the plot and the vectors also demonstrate this flow behaviour.

In Figure 67 the contour plot of the magnitude of the average velocities in the storage area is present. Moreover vectors are added to indicate the water flow in x- and y-direction. Furthermore, some important structures of the model are plotted in this figure: the left bank, the turbine intakes, the separation wall, the elevated floor to the turbine intakes and the right bank.

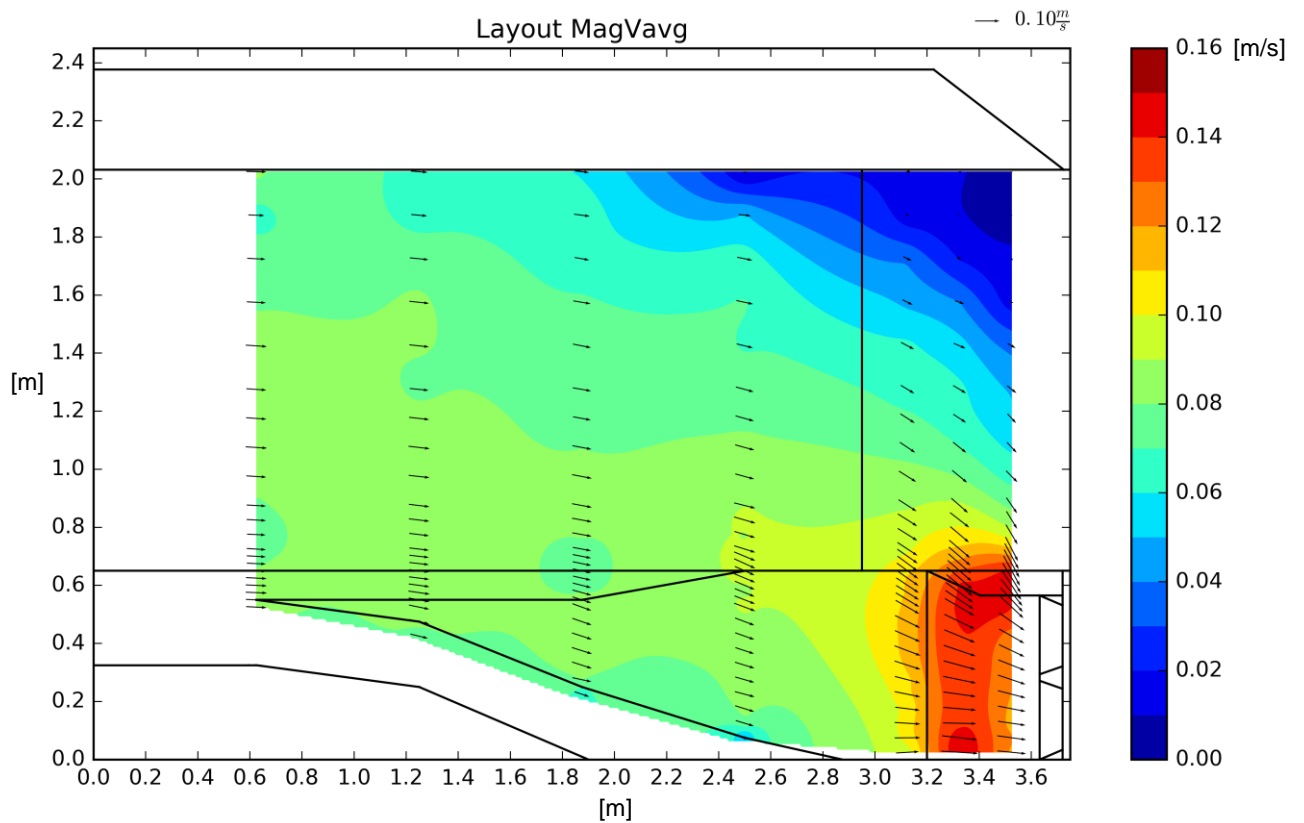


Figure 67: Magnitude of the average velocities in storage area

In Figure 68 the contour plot of the magnitude of the average velocities is superimposed over the drawing of the storage area. The flow conditions and the distribution across the whole upstream area can be seen in comparison to the model structure. Also the positions of the cross sections are present.

6. Conclusion and perspective

6.1 Conclusion

The aim of this thesis is the investigation of the the approach flow behaviour to the turbines at the model Gratkorn by means of ADV-measurements. The water flow velocity measurements with the Acoustic Doppler Velocimeter deliver very interesting and valuable results. Even in areas with turbulences and fast changing velocities (high gradient) in different directions the device works excellent and the outcome in these regions is impressive. The whole upstream storage area is investigated and the flow distribution for every cross section is determined. The result is a very complex flow distribution in the region near the turbine intakes and the separation pillar with high velocities in all directions. In this area the flow to the turbines, especially to turbine 2, is not uniform. Even though the structures in the area have been modified a several times the outcome is unsatisfactory and further development is needed to generate a uniform and steady water flow towards both turbines. Further away from the turbine intakes the influence of the separation wall is insignificant and the water flow distribution gets increasingly uniform. A significant influence of the inlet area and the separation wall architecture is noticed as far as 50 m upstream from the weir axis. The velocities in flow direction are dominant and nearly equal in size across the whole cross section. Further away from the turbine intakes there is nearly no influence of the structure recognisable. The flow distribution is similar to the distribution in a straight river with a trapezoidal river bed.

6.2 Perspective

Measurements in laboratory models are a good instrument to understand and predict water flows in the prototype. Although the measurements are very precise and reliable they are just one part of a hydraulic investigation on certain problems. This thesis is a first approach on Acoustic Doppler Velocity measurements in a storage area of a low head run-off hydropower plant model. The objective is a suitable architecture of the underwater structures near the turbine intakes. This should guarantee a mostly undisturbed and steady approach flow towards the turbines under different load cases.

Further subsequent steps can be:

- A comparison of the results to the numerical calculation including identification of deviations and the reason of their occurrence.
- The investigation of the flow behaviour with different load cases. In this thesis the water flow at normal operation conditions (both turbines working under full load, storage level reached) is examined. Further load cases can be a flood event or the revision or failure of one turbine.
- The investigation of different hydropower plants and a comparison of the results.

List of references

- [1] Hydraulic Engineering and Water Resources Management (May 2017):
<https://www.tugraz.at/en/institutes/iwb/research/modelling/laboratories/>
- [2] New World Encyclopedia, Doppler effect (May 2017):
http://www.newworldencyclopedia.org/entry/Doppler_effect
- [3] Wikipedia The Free Encyclopaedia, Doppler effect (May 2017):
https://en.wikipedia.org/wiki/Doppler_effect
- [4] Wikipedia Die freie Enzyklopädie, Doppler-Effekt (May 2017):
<https://de.wikipedia.org/wiki/Doppler-Effekt>
- [5] Wikipedia The Free Encyclopaedia, Acoustic Doppler Velocimetry (May 2017):
https://en.wikipedia.org/wiki/Acoustic_Doppler_velocimetry
- [6] Nortek AS, Vectrino (May 2017): <http://www.nortek-as.com/en/products/velocimeters/vectrino>
- [7] Nortek AS, Vectrino Profiler (May 2017): <http://www.nortek-as.com/lib/user-seminars/ketil-horn-vectrino-profiler>
- [8] Nortek AS, Doppler Velocity Measurement (May 2017):
<http://www.nortekusa.com/usa/knowledge-center/table-of-contents/doppler-velocity>
- [9] Nortek AS, Acoustic Doppler Velocimeters (May 2017):
<http://www.nortekusa.com/usa/knowledge-center/table-of-contents/velocimeters>
- [10] Palmer (2002): Acoustic Doppler Velocimetry, Part I: Principles of Operation
- [11] ARGE Gratkorn (2009): Wasserkraftwerk Gratkorn, Kurzbeschreibung des Vorhabens
http://www.umwelt.steiermark.at/cms/dokumente/11262212_9176022/52e69129/KW%20Gratkorn%20Kurzbeschreibung%20Vorhaben.pdf

- [12] VECTRINO application help
- [13] Nortek AS (2004): Vectrino Velocimeter User Guide
- [14] Nortek AS (2012): Vectrino II, A profiling bi-static acoustic velocimeter
<http://www.nortek-as.com/lib/technical-notes/doppler-velocimeter-comparison/view>
- [15] Nortek AS (2013): Nortek Quick Guide Vectrino Velocimeter
- [16] Nortek AS (2017): Datasheet Vectrino Lab 01-2017, <http://www.nortek-as.com/lib/data-sheets/datasheet-vectrino-lab/view>
- [17] Béla Sokoray-Varga, (2014). Messungen mit dem Vectrino. IWG Institut für Wasser- und Gewässerentwicklung, Karlsruher Institut für Technologie Verena Höger, BAW Bundesanstalt für Wasserbau, Karlsruhe im November 2014
- [18] Chanson, H., Trevethan, M., & Aoki, S. I. (2008). Acoustic Doppler velocimetry (ADV) in small estuary: field experience and signal post-processing. *Flow Measurement and Instrumentation*, 19(5), 307-313.
- [19] Cea, L., Puertas, J., & Pena, L. (2007). Velocity measurements on highly turbulent free surface flow using ADV. *Experiments in Fluids*, 42(3), 333-348.
- [20] Castillo, L. G., & Carrillo, J. M. (2014). Velocities measurement in highly turbulent and aerated flows.
- [21] Martin, V., Fisher, T. S. R., Millar, R. G., & Quick, M. C. (2002). ADV data analysis for turbulent flows: Low correlation problem. In *Hydraulic Measurements and Experimental Methods 2002* (pp. 1-10).
- [22] Castillo, L. G. (2009). Filtering and validation of velocities obtained with ADV equipment inside of hydraulic jumps. In *International Workshop on Environmental Hydraulics, IWHE, Valencia, Spain*.

- [23] Wahl, T. L. (2000). Analyzing ADV data using WinADV. In Building Partnerships (pp. 1-10).
- [24] Wahl, T. L. (2002). Win ADV User's Manual, Water Resources Research Laboratory, Denver, Colorado
- [25] Schneider, J. (2015). Versuchstechnik und Laborübungen im Wasserbau, Vorlesungs- und Übungsskriptum, Institut für Wasserbau und Wasserwirtschaft, Graz, Austria

List of figures

Figure 1: Laboratory model Gratkorn	2
Figure 2: Doppler effect [2].....	3
Figure 3: Velocimeter [9]	4
Figure 4: Acoustic sensor [9].....	5
Figures 5 and 6: Original ADV [7].....	5
Figure 7: Vectrino side-looking probe [6].....	7
Figure 8: Datasheet Vectrino lab side-looking probe [16].....	8
Figure 9: Vectrino side-looking probe indicator [17]	8
Figure 10: Vectrino components [7]	9
Figure 11: Vector v [14].....	11
Figure 12: Maximal SNR [7]	12
Figure 13: Vectrino Sweet Spot [7].....	13
Figure 14: Control panel – accurate measurement	14
Figure 15: Configuration panel.....	15
Figure 16: Correlation very high	17
Figure 17: Correlation not high enough.....	18
Figure 18: Inaccurate measurement	19
Figure 19: No Acoustic Interference [14].....	21
Figure 20: Acoustic Interference [14]	22
Figure 21: Interference problem.....	22
Figure 22: Solution of Acoustic Interference Problem [14]	23
Figure 23: Probe check	24
Figure 24: Control panel WinADV software.....	27
Figure 25: Options panel WinADV software	29
Figure 26: Correlation Filter [21].....	30

Figure 27: Raster glass channel.....	33
Figures 28 and 29: Installation of the Vectrino+	34
Figures 30 and 31: Vectrino+ in application	35
Figure 32: Velocities in x-direction in flume	37
Figure 33: Magnitude of average velocities in flume	37
Figure 34: Velocities in x-direction in flume masked	38
Figure 35: Point L4PH.....	39
Figure 36: Location plan KW Gratkorn [11]	42
Figure 37: Layout model Gratkorn [TU Graz]	44
Figure 38: Layout turbine 2 [TU Graz, modified]	45
Figure 39: Longitudinal section turbine 2 [TU Graz, modified].....	46
Figure 40: Section sediment control bedplate [TU Graz, modified]	47
Figure 41: Picture model Gratkorn	48
Figure 42: Layout model Gratkorn with cross sections [TU Graz, modified].....	49
Figure 43: Cross section turbine 1 and 2 (dimensions in cm)	50
Figure 44: Velocities in x-direction at turbine 1.....	51
Figure 45: Magnitude of average velocities at turbine 1	52
Figure 46: Point D4	54
Figure 47: Velocities in x-direction at turbine 2.....	55
Figure 48: Magnitude of average velocities at turbine 2.....	56
Figures 49, 50, 51 and 52: Cross sections PR A-OW, PR B-OW, PR 0.1-O and, PR 1.0-OW	59
Figures 53 and 54: Velocities in x-direction and magnitude of V-average at profile PR A - OW	61
Figures 55 and 56: Velocities in x-direction and magnitude of V-average at profile PR B - OW	64

Figures 57 and 58: Velocities in x-direction and magnitude of V-average at profile PR 0.1 - OW.....	67
Figures 59 and 60: Velocities in x-direction and magnitude of V-average at profile PR 1.0 - OW.....	70
Figures 61 and 62: Velocities in x-direction and magnitude of V-average at profile PR 1.1 - OW.....	73
Figures 63 and 64: Velocities in x-direction and magnitude of V-average at profile PR 2.0 - OW.....	76
Figures 65 and 66: Velocities in x-direction and magnitude of V-average at profile PR 2.1 - OW.....	79
Figure 67: Magnitude of the average velocities in storage area.....	82
Figure 68: Velocity distribution in storage area	83

List of tables

Table 1: Critical distances to solid surfaces [17]	23
Table 2: Measurement time for each point in the flume to get mean velocity... 40	
Table 3: Max. and min. velocities turbine 1	53
Table 4: Max. and min. velocities turbine 2	57
Table 5: Max. and min. velocities profile PR A - OW.....	62
Table 6: Max. and min. velocities profile PR B - OW.....	65
Table 7: Max. and min. velocities profile PR 0.1 - OW	68
Table 8: Max. and min. velocities profile PR 1.0 - OW	71
Table 9: Max. and min. velocities profile PR 1.1 - OW	74
Table 10: Max. and min. velocities profile PR 2.0 - OW	77
Table 11: Max. and min. velocities profile PR 2.1 - OW	80

Appendix

The attached DVD contains:

1. Measurement data of all points of every cross section in the laboratory flume and the model Gratkorn.
2. Cross section plans in a certain scale for:
 - a. Laboratory flume
 - b. Intake Turbine 1
 - c. Intake Turbine 2
 - d. Profile PR A – OW
 - e. Profile PR B - OW
 - f. Profile PR 0.1 - OW
 - g. Profile PR 1.0 - OW
 - h. Profile PR 1.1 - OW
 - i. Profile PR 2.0 - OW
 - j. Profile PR 2.1 - OW
 - k. Profile PR 2.2- OW
3. Longitudinal section plans in a certain scale of:
 - a. Turbine 2
 - b. Weir field B
 - c. Separation pillar
4. Layout plans in a certain scale for:
 - a. Turbine 2

- b. Model Gratkorn
 - c. Upstream water area model Gratkorn
5. Plots of calculation of the average velocity according to the final mean in the flume for all 81 points and at the inlet of turbine 2 for five more points.
6. Contour plots of velocities (V_x , V_y , V_z , AvgVmag and VmagAvg) for the laboratory flume.
7. Contour plots of velocities (V_x , V_y , V_z , AvgVmag and VmagAvg) for the model and the prototype for:
 - a. Intake Turbine 1
 - b. Intake Turbine 2
 - c. Profile PR A – OW
 - d. Profile PR B - OW
 - e. Profile PR 0.1 - OW
 - f. Profile PR 1.0 - OW
 - g. Profile PR 1.1 - OW
 - h. Profile PR 2.0 - OW
 - i. Profile PR 2.1 - OW
 - j. Profile PR 2.2- OW
 - k. Layout upstream area
8. A txt-file with the used Python codes for the calculation of the average velocity according to the final mean.
9. A txt-file with the used Python codes for the creation of the contour plots for the model and the prototype.